UNIVERSITÀ DEGLI STUDI DI TRIESTE

XXXI CICLO DEL DOTTORATO DI RICERCA IN

NANOTECNOLOGIE

APPLICATION OF NANOTECHNOLOGY TO THE DIAGNOSIS AND TREATMENT OF ORAL AND OROPHARYNGEAL CANCER

Settore scientifico-disciplinare: **MED/31**

DOTTORANDA
MARGHERITA TOFANELLI

COORDINATORE
PROF. ALBERTO MORGANTE

SUPERVISORE DI TESI
PROF. GIANCARLO TIRELLI

CO-SUPERVISORE DI TESI
PROF. ROBERTO DI LENARDA

ANNO ACCADEMICO 2018/2019

INDEX

1. Abstract

In head and neck oncology, the oncogenic viral role is currently debated. Particularly, the infection by Human Papillomavirus (HPV) demonstrated oncogenic properties in the development of oropharyngeal cancers.

Nowadays there are no recommended or validated methods to screen for early cases of HPV-driven oropharyngeal cancer. The present work developed and tested in vitro and in vivo performance of an innovative methods to early detect HPV-positive (HPV+) oropharyngeal squamous cell carcinoma (OPSCC). This system is represented by a biosensor for the detection of HPV antibodies against HPV E6 and E7 oncoproteins using the Electrochemical Impedance Spectroscopy (EIS) technique. Assays to quantify HPV-specific antibodies were based on Enzyme Linked Immuno-Sorbent Assays (ELISA); ELISA requires specialized laboratory and personnel, it is quite expensive, complex and time-consuming. Moreover, it requires pre-steps of sample processing, that can cause proteins denaturation and bioactivity modification.

An instantaneous self-test would be particularly useful to detect the presence of HPV antibodies in blood, both for diagnostic and prognostic purposes. A cheap test could really impact on developing countries in the context of cancer prevention.

The work is composed of three parts:

1. development of a biosensor based on gold screen-printed electrode (Au-SPE) functionalized with self-assembled monolayer (SAM) s and a commercial mixture of E7 peptides (PepMix) acting as the antigen to capture serum antibodies;

2. the second part of the work was focused on the recombinant production of E6 oncoproteins and a different electrode functionalization using hybrid SAMs.

3. the last part reported the analysis of biological samples testing the device in different conditions.

2. Introduction

Head and neck squamous cell carcinomas (HNSCC) include a various group of malignant cancers arising from the upper aerodigestive tract. The subsites of HNSCC comprise the oral cavity, nasopharynx, oropharynx, hypopharynx, and larynx.

HNSCCs collectively represent the sixth most common malignancy worldwide, accounting for 932,000 new cases and 379,000 deaths in 2015 [1].

Over the past four decades, unusual epidemiological trends have been observed in HNSCC.

Incidence rates of tumours arising from non-oropharyngeal subsites (oral cavity, hypopharynx and larynx) have diminished while the incidence of oropharyngeal squamous cell carcinoma (OPSCC) has gradually increased [2].

These subsite-specific epidemiological trends have been ascribed to modifications in common factors that have resulted in changes in exposure to two groups of risk factors: (a) tobacco and alcohol consumption and (b) Human PapillomaVirus (HPV) infection.

HPV is the most common sexually transmitted infection in the United States and the primary infectious cause of HNSCC [3] High-risk HPV infection has a widespread diffusion, but most people can eradicate the virus [4], so the development of HPV-associated malignancies requires a persistent infection.

The oropharynx shows the strongest predisposition to HPV, that HPV-positive OPSCC is accepted as a different neoplastic entity with a distinctive molecular, histopathological epidemiological, and clinical profile [5,6]. Patients with HPV-positive OPSCC differ from the traditional profile of HNSCC patients in that they are often younger than 60 years in age and usually with no history of heavy tobacco and alcohol use [6]. HPV-positive OPSCC also shows higher sensitivity to treatment and a significantly better prognosis than HPV-negative HNSCC [5], tendencies which have led to the publication of a staging system dedicated to this tumour [7] and changes in treatment strategies [8].

Despite progresses reached in diagnosing cases of HPV+ OPSCC in pre-clinical settings, there are still a lot of challenges in clinical settings and there are no recommended or validated methods to screen for early stages of HPV + HNSCC.

2.1 Human papillomaviruses

Papillomaviridae is a family of non-enveloped viruses with a circular double-stranded DNA genome [9].

Firstly, Papillomavirus was classified on the nucleotide sequence of the major structural protein L1: different Papillomavirus types shared less than 60% identical L1 nucleotide sequences to the other types [10]. In 2004 De Villers et al.[11], introduced an alternative phylogenetic classification, considering the genomic sequence differences but also biologically features like host species, target tissue, and virus pathogenicity using a nomenclature of genera based on the Greek alphabet.

Generally, human papillomaviruses (HPV) are divided in five different evolutionary genera (Alpha, Beta, Gamma, Mu and Nu) that differ for DNA genome sequence, life-cycle characteristics and disease associations (**Figure 1**). Alpha papillomavirus group is divided in cutaneous and mucosal subtypes: cutaneous types commonly infect the skin of the hands or feet; mucosal types instead infect the epithelium of vaginal tract, oropharyngeal tract and anogenital zone. Within this group, approximately 200 genotypes have been described based on viral genome sequence [12] and they are divided into two subgroups based on the oncogenic ability: low-risk and high risk types. Normally, low-risk (LR) HPVs cause only infections, while high-risk HPV infections are associated with cancers. Among these high-risk HPV types, HPV 16, 18, 31, 33, 45, 51, 52, 56, 58, and 59 and 6 low-risk HPV types (11, 32, 44, 53, 57, and 81), have been identified in HNSCC tumors [13]. Among the HR-HPV types involved in head and neck carcinogenesis, HPV16 is the most common viral cause of HNSCC and is identified in at least 87% of HPV-positive OPSCC [14,15].

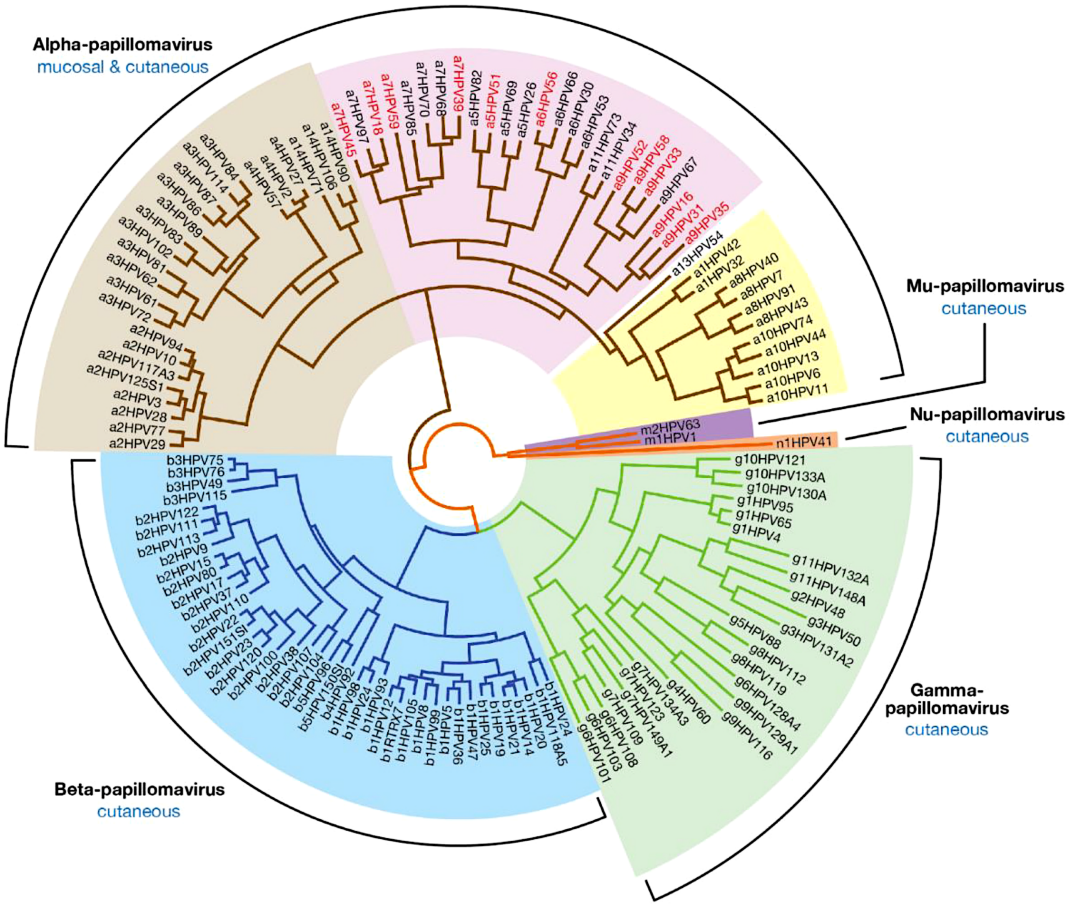

Figure 1. Phylogenetic tree illustrating the relationship between Human Papillomaviruses. HPVs comprise five evolutionary genera, indicated by a Greek letter, different for epithelial tropism and disease association. In particular the Alpha papillomavirus group include the low-risk mucosal type, involved in genital warts formation, and the high-risk mucosal type, considered as the main etiological cause of cervical neoplasia and cancer. Image reprinted from Doorbar et al [16], with permission from Elsevier copyright license (2019) n.4661841432952.

2.2 HPV structure and viral proteins

The genome is made of approximately 8 kilobases, encoding 8 open reading frames (ORFs) that enable viral genome replication and viral particle assembly [17]. The genome is divided in three functional regions: the long control region (LCR) of ~1 kb, that is a a noncoding regulatory region containing biding sites for different cellular transcription factors and

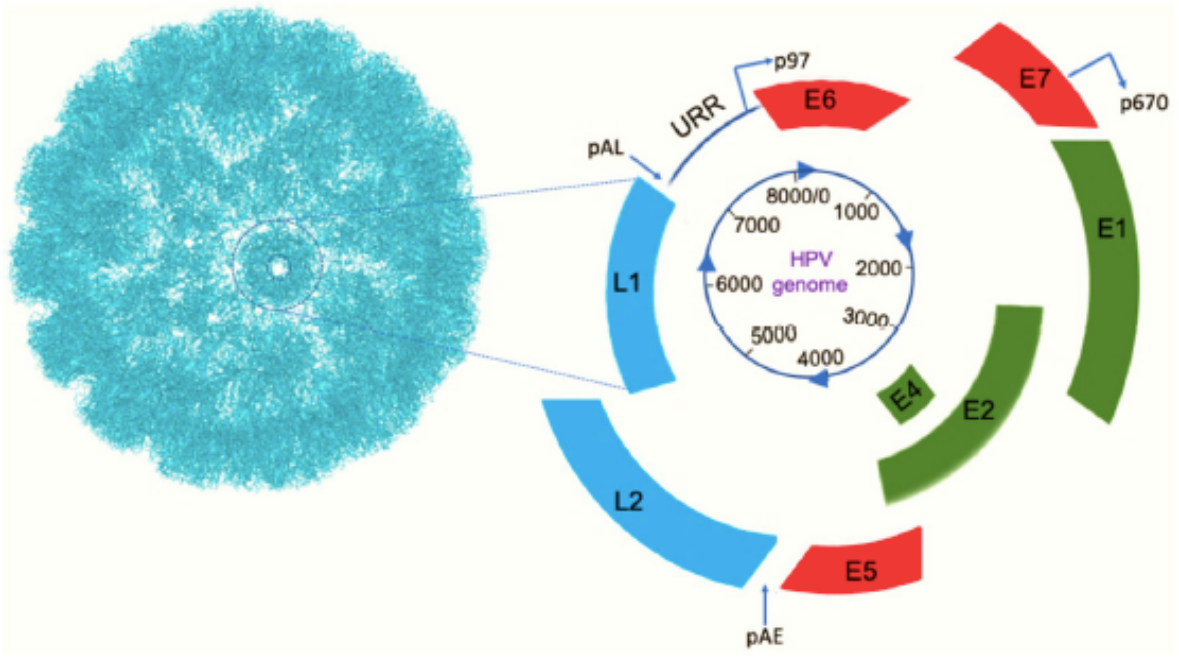

Figure 2. A schematic of the genome of HPV16 and capsid proteins. Right panel: E1, E2, E4, E5, E6, and E7 are genes that code for early proteins in red and green colours; E5, E6, and E7 are oncogenes. L1 and L2 (capsid proteins) are genes that code for late proteins, shown in light blue colour. URR (upstream regulatory region) contains origin of replication, enhancer elements, and early promoter (p97); URR controls viral replication. p670 is the late promoter. pAE and pAL are early polyadenylation and late polyadenylation sites, respectively. Left panel: The L1 protein forms pentamers (one is circled) and each pentamer has an L2 protein at its centre (not shown). Seventy-two copies of the pentamers assemble to form an icosahedral capsid. Image reprinted from Tumban 2019 [18].

for viral protein E1 and E2 [18]; then, early (E1, E2, E4, E5, E6, and E7) and late (L1 and L2) genes, based on the timing of expression with respect to the viral life cycle [16]. The ~4 kb early (E) region encodes for non-structural proteins (E1, E2, E4, E5, E6 and E7) involved in viral replication and oncogenesis; the ~3 kb late (L) region encoding for the two structural proteins (L1 and L2) forming the viral icosahedral capsid, about 55 nm in diameter, that protect the viral genome inside [19]. In particular, the E1 viral helicase and E2 DNA-binding protein directly mediate viral genome replication and amplification, while E4, E5, E6, and E7 are accessory proteins that coordinate viral genome amplification and virulence. On the other hand, the late genes L1 and L2 encode viral capsid proteins necessary for the final stages of virion assembly and mediate viral entry into future host cells.

Following HPV infection, the genome is maintained as an episome in the nucleus; integration of E6 and E7 into the host chromosome and persistent expression of these oncogenes interferes with the functioning of cell cycle regulator (tumour suppressor) proteins.

E1 and E2 are essential proteins for the viral initial amplification phase. E2 is a sequence specific DNA binding protein that directs the main transcription regulator of the papillomaviruses [20]. E2 can engage cellular factors to viral genome, activating or repressing the transcriptional process; additionally, it can recruit also the viral E1 protein in the viral replication origin activating viral genome replication [16,21]. E2 plays also a role in viral genome segregation during the mitosis, tethering viral genome to the host chromosomes for the retention, maintenance and viral genome partitioning [21]. Moreover, E2 can cause cells growth arrest and senescence suppressing the early viral promoter and so down regulating the E6 and E7 expression. E2 has a short half-life and it is regulated by multiple factors; occasionally the protein functions can be interrupted by mutation or integration of the viral genome into the host genome, leading to an uncontrolled expression of E6 and E7 genes and consequently to the carcinogenesis [21].

E4 and E5 also contribute to viral genome replication, modifying cellular environment; E5 is a transmembrane protein with pore-forming capability and can interfere with apoptosis and intracellular vesicles trafficking [22]. E5 protein is involved in *koilocytes* formation: these elements are epithelial cells with hyperchromatic nuclear enlargement surrounded by cytoplasmic vacuolization. This cytopathic effect is detected by the pathologists to identify and describe HPV infected cells in cytologic specimens [23]. E4 is synthetized fused with E1 and then spliced by E1^E4 transcripts, in fact the first few amino acids derived from the N-terminus of E1 [24]. E4 is commonly present in upper epithelial layers and contributes in virus release and transmission: it interrupts the keratin composition compromising the normal cornified structure of the mucosa [16]. E6 and E7 are two well-known HR-HPVs oncoproteins and the main actors of the uncontrolled cells proliferation and neoplastic transformation [18]. High- and low-risk HPV E6 and E7 proteins present some functional differences that distinguish their cellular transformation ability. In low-risk HPV infection the basal epithelial cells proliferation is mainly regulated by cellular growth factors, like in the uninfected epithelium; E6 and E7 roles in these lesion types is to stimulates the cell cycle in the upper epithelial layers allowing viral genome amplification. In high-risk infection, instead, E6/E7 expression induces cell cycle entry and cell proliferation in basal and middle epithelium layers causing a neoplastic transformation: E7 displaces the transcription factors E2F4 and E2F5 from the

retinoblastoma protein (pRb), without needing the pRb phosphorylation, and E6 associate with E6AP (E6 associated protein) mediates the ubiquitination and proteasomal degradation of p53 [16]. In particular, the activity of E6 proteins is to bind to p53 and induce ubiquitin-dependent proteolysis of the p53 tumour suppressor protein. P53 is a regulator of the DNA-damage response, the G2/M cell cycle transition and it represents the most commonly mutated tumour suppressor gene in cancer [17]. It is important to know that only E6 from HR-HPV can bind p53 and the affinity of this binding correlates with the oncogenic potential; this feature explains why different HPV types cause neoplastic transformation with different strength [25].

E7 oncoprotein exercises the oncogenic potential by inducing the proteolysis of Retinoblastoma (Rb)-family tumour suppressors. Rb inhibits the cell cycle by regulating the accumulation of E2F and it controls te G1 to S-phase cell cycle transition. E7 increases the degradation of Rb protein by way of an ubiquitin-proteasome pathway [17]: the Rb degradation discharges E2F family mitogenic transcription factors into the nucleus, activating S-phase and triggering proliferative transcriptional programs. Degradation of Rb also releases CDKN2A gene expression, which codes for the tumour suppressors p14ARF, as well as p16INK4A, a surrogate marker of HPV-driven oropharyngeal cancers [26]. E7 belonging to low risk HPV interacts with Rb at a lower affinity that is not sufficient to cause Rb degradation thus promoting oncogenesis.

2.3 HPV infection mechanism

The keratinocyte progenitors are the host cells for HPV. They are situated in the basal layer of stratified squamous epithelia and close to the basement membrane. We know that the infection need viral access to the basement membrane [27]. In the anogenital tract and in the cervix, the virus accesses to basal cells through interruptions of the mucosa due to mechanical micro-abrasions occurred during sexual contacts. Differently, the oropharyngeal histologic structure permits the HPV infection without any epithelial abrasion. In fact, the oropharynx is formed by the set of palatine, lingual, tubal and adenoid tonsils that are all lymphoid structures known as “Waldayer’s ring”.

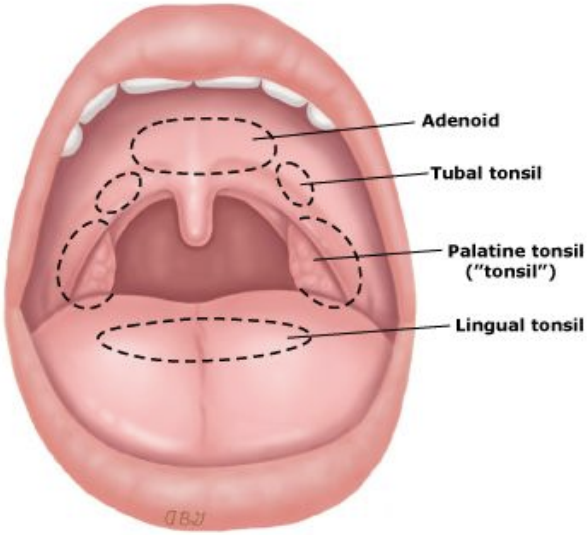

Figure 3. Oropharynx includes adenoid, tubal, palatine and lingual tonsils. These lymphatic structures are collectively named "Waldeyer's ring".

Waldeyer's Ring's components are characterized by a specialized squamous epithelium that is fenestrated and infiltrated with lymphoid tissue. This epithelium is called reticulated because it is a sort of mesh in which the basement membrane is discontinuous; these interruptions represent a natural passage to basal keratinocytes in the absence of traumatic epithelial disruption, permitting contact between immune cells and oral antigens [28].

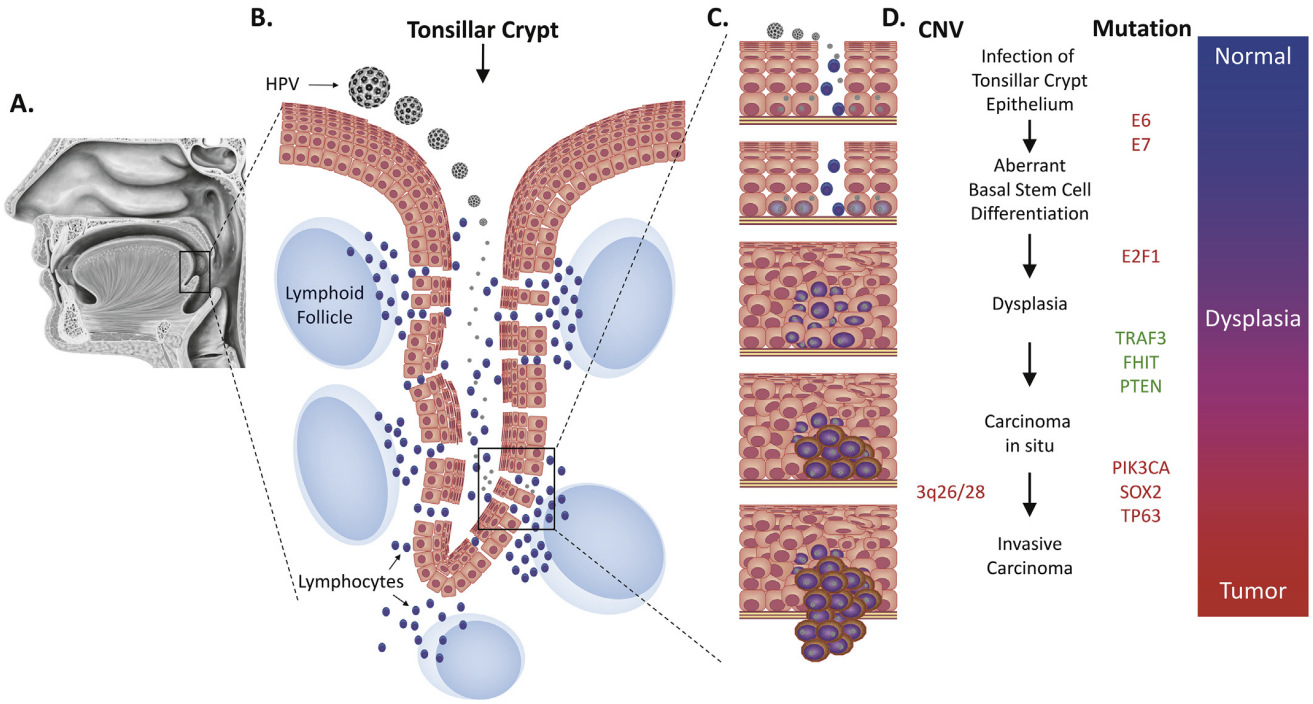

Figure 4. Tumor progression model for HPV-related carcinogenesis. (A) In the head and neck, HPV showed tropism for lymphoid-associated structure of the oropharynx (area in black box). (B) HPV accesses to basal keratinocyte progenitors

through interruptions in the reticulated epithelium of the tonsillar crypts. (C) Infection of the tonsillar epithelium result aberrant basal cell differentiation, dysplasia, carcinoma in situ, and finally invasive carcinoma. (D) Hypothetical somatic mutations in a multistage tumor progression model. Genes and loci in red are upregulated or activated or show increase in copy number. Genes in green undergo loss of function mutation or deletion. CNV, copy number variations.

This peculiar property of Waldeyer's ring may explain the high tendency of HPV to cause squamous cell carcinoma in oropharynx [17].

Once the virus has reached the basal keratinocyte, it binds elements in the extracellular matrix. The capsid proteins trigger conformational changes in L1 and L2 that transfer virion particles to the host, necessary for viral incorporation.

Once viral entry and uncoating occurred, the HPV-DNA is transferred to the nucleus in form of *episome:* this is a distinct element from the host cell genome, that uses host cell enzymes to replicate itself along with the host and it is maintained at low-copy number [29].

Keeping low-copy replication of the genome, HPV can escape the host immune system. E6 and E7 are expressed before viral replication, leading cell cycle entrance and cell proliferation. The dysregulation of the cell cycle induced by E6 and E7, represents the first step to carcinogenesis.

Normally, only basal keratinocyte stem cells can proliferate; HPV-encoded genes alter key keratinocyte differentiation and proliferation pathways to prefer virus production
and viral life cycle completion. In high-risk HPV types, these perturbations predispose cells to neoplastic transformation [17].

2.4 Molecular biology of HPV-related OPSCC

The two main oncoproteins in HPV-related OPSCC are E6 and E7. E6 alters p53 activity while E7 induces pRb degradation releasing E2F transcription factor [30]. Due to E7 activation, p16INK4a is overexpressed and released from the inhibitory activity of the pRb/E2F complex, allowing epithelial cells to avoid oncogene-induce senescence and to activate survival signalling pathways [31].

p16 INK4a overexpression becomes crucial for cell survival in HPV-driven tumours, while it is frequently unexpressed in HPV non-related tumours. This makes the p16INK4a
overexpression an indirect marker of transcriptionally active HPV in oropharyngeal carcinogenesis [32]. However, the identification of HPV-driven OPSCC should be complemented with the detection of viral DNA to avoid misclassification of some HPV-negative cases in which p16INK4a expression

can be present as well. E6/E7 expression is associated with chromosomal instability that enhances the risk of genomic alterations, the suppression of apoptotic pathway and a rise of telomerase activity [33]. The activity of other proteins (E1, E2, E3, E4 and E5) is essential to complete the viral cycle but it is not essential to trigger oncogenic transformation.

2.5 Clinical and histopathological differences between HPV-related and non-HPV-related OPSCC.

The importance to early recognize the HPV infection in OPSCC is due to the different clinical and histopathological behaviour that this class of tumour shows compared to not-HPV-driven OSCC.
The differences are such expressed that the 8th edition of Tumour Neck Metastasis (TNM) staging system published by American Joint Committee on Cancer (AJCC) introduced a dedicated classification for HPV-related OPSCC [7]. (data are summarized in Table 1).
It is curious to note that HPV-related OPSCC cases are defined as p16INK4a-positive patients and no other biomarkers have been used to classify this group.

	HNSCC HPV-non related	HNSCC HPV-related
Risk factor	Alcohol, tobacco	Number of oral sex partners
Age	Older	Younger
Incident trends	Mostly decreasing	Increasing
Head and neck tumor location	Anyone	Base of the tongue, tonsil
Stage	Anyone	Small T, large N involvement
Radiological image	Anyone	Cystic nodal involvement
Histopathological features	Keratinising	Baseloid, Non-keratinising
Tumor differentiation	Anyone	Undifferentiated
Biology and genetic alterations:		
CDKN2A	Common	Rare
$p16^{INK4a}$ overexpression	Rare	Common
EGFR	Common (amplification)	Rare
p53	Common	Rare (p53 degradation by E6)
pRb	Rare	Rare (pRb degradation by E7)
PIK3CA	Common	Common (APOBEC)
TRAF3	Rare	Common
Outcomes	Worse OS and PFS	Better OS and PFS
Metastatic dissemination	Yes	Rarely
Comorbidity	Yes	No
Second primary tumors	Yes	No
Prevention strategies	Quitting smoking and drinking	Vaccination (in development)

HNSCC, head and neck squamous cell carcinoma; HPV, human papillomavirus; OS, overall survival; PFS, progression free survival.

Table 1. Main differences among patients with HPV-related and non-related head and neck squamous cell carcinoma [31]

It is also important to note that HPV-related OPSCC are generally diagnosed in advanced stages, with a small tumour size (T) but great nodal metastasis (N) [34].

Histopathological features of HPV-related OPSCC usually are non- non-keratinizing, undifferentiated or basaloid and second primary neoplasms are usually less expressed, probably because tobacco or alcohol use (the most common other risk factors) are not frequent in this category [35].

In addition, active HPV is not present in the mucosa just close to the primary tumour, meaning that the so-called "field cancerization" phenomenon lacks in this type of tumours [36].

The primary tumour is usually composed of many nests of cells with scarce cytoplasm, hyperchromatic nucleus with high mitotic activity and low squamous maturation. The lymphatic infiltrate is generally high and distinctive. The morphologies can variate among papillary, adenosquamous, lymphoepithelial and spindle cell types. Due to the atypical morphology with no maturation, no keratinisation and high level of mitosis, a grade is not assigned to this class of tumours [37].

The imaging describes that HPV-related OPSCC have well-defined borders, very frequently cystic nodal involvement and could have small or even occult primary tumours [31].

Clinical and pre-clinical studies supported that HPV-related OPSCC are more radiosensitive than non-related ones [5,8]. This tendency results in a more favourable prognosis and it seems a result of E6 and E7 activities: HPV-positive cells fail to resolve radiation-induced double strand breaks, increasing their intrinsic radiosensitivity. In fact, apoptosis signalling after radiation is higher in HPV-related OPSCC, probably due to the activation of a basal fraction of wild-type p53 (that is only inhibited by E6 but not mutated), which is not present in HPV-negative tumours showing p53 somatic mutations [31]. Moreover, p16INK4a damages homologous recombination DNA repair through the downregulation of cyclin D1, and this could explain the prognostic and predictive value of p16INK4a overexpression in OPSCC.

Radiosensitivity is influenced by many other molecular and environmental factors, such as a high tissue hypoxia signalling that makes radio-resistant HPV-negative cancers; moreover E6 and E7 oncoproteins activate immune system response with the result of an higher immune infiltration than in HPV-negative cases and this seems to be connected with an increased radio-sensitivity [38].

2.6 HPV detection techniques

Nowadays HPV testing is mandatory for an accurate OPSCC diagnosis, management and prognostic stratification. There are several available techniques with different sensitivity and specificity rates;

standalone or combinations of the following tests are existing to improve identification of viral presence: p16 immunohistochemistry (IHC), HPV-DNA in situ hybridization (ISH), E6/E7 HPV-RNA ISH, HPV-DNA polymerase chain reaction (PCR) and E6/E7 HPV real time- polymerase chain reaction (RT-PCR) [39].

E6/E7 HPV-mRNA evaluation is considered the gold standard to confirm viral oncogenesis since it detects oncogene transcriptional active HPVs. Comparison of main HPV detection techniques are summarized in Table 2.

Method	Description	Advantages	Disadvantage
E6/E7 HPV mRNA RT–PCR	–Detection of messenger RNA E6/E7 HPV –HPV type-specific	–GOLD STANDARD: high sensitivity and specificity –Detects transcriptionally active HPV	–Difficult to reproduce on a clinical setting
$p16^{INK4a}$ IHC	–Surrogate marker of E7 HPV	–Easy and most implemented technique on clinical setting –High sensitivity –In HPV presence, greats indications of transcriptional activity	–Moderate specificity –Not concordance rates to the gold-standard outside the oropharynx –Not exclusive from HPV related tumors
HPV DNA PCR	–Amplification of conserved regions of the HPV genome	–Based of PCR technique, available in multiple hospitals –qPCR quantitative test: most sensitive method for HPV DNA detection and indicates viral load –Different commercial set available –HPV type-specific	–Indicates an HPV infection that may be transient –Easy contamination –Low specificity –Sensitivity and specificity of the technique vary depending on the sets of primers used
HPV DNA ISH	–Detection and location of HPV in tissue or cells	–High specificity –Simple and accessible –Allow to distinguish episomal and integrated HPV DNA –HPV mRNA ISH also available, with high sensitivity and specificity despite quantity of viral load	–Low sensitivity when low viral load

IHC, immunohistochemistry; ISH, *in situ* hybridization; HPV, Human papillomavirus; qPCR, quantitative polymerase chain reaction; RT-PCR, reverse transcriptase polymerase chain reaction.

Table 2: Main Human papilloma virus detection techniques [31].

Combination testing should increase the sensitivity of HPV detection but can results in a disagreement between tests increasing costs. In early 2018, an evidence-based consensus recommended HPV testing in oropharyngeal cancers regardless of morphology and it did not recommend routinely testing other head and neck subsites [40].

2.6.1 P16 immunohistochemistry

p16 is a tumour suppressor protein encoded by the CDKN2A gene (cyclin dependent kinase inhibitor 2A) and normally it prevents damaged cells from proliferating by inhibiting the activation of Rb [37]. Thus, degradation of Rb that is mediated by the E7 oncoprotein, causes the overexpression of p16.

For these reasons, p16 expression detected using immunohistochemistry is a highly sensitive substitute marker for transcriptionally active HPV infection [41].

Thus, the p16INK4a expression is a surrogate marker of HPV involvement and it is the most widely implemented technique in the clinical setting because it shows a high sensitivity (90%) and moderate (>80%) specificity [40]. The technique is cost effective, can be performed on formalin fixed, paraffin embedded (FFPE) tissues and cytology cell block. The main advantage of IHC is the excellent kappa scores for interobserver consistency, making the p16 immunostaining easy to interpret [40,42]. The high sensitivity is due to the lack of connection between the p16 upregulation and the HPV subtypes, so p16 immunohistochemistry represents the most practical test available for this purpose.

However, the use of IHC alone is quite questionable. There is 25% of discordant cases, mostly p16INK4a- positive and E6/E7 HPV mRNA-negative. In addition, there are variations among studies in the definition of p16INK4a overexpression [31]. A recent meta-analysis shows that the combination of p16INK4a IHC with HPV DNA detection allows to reach the highest specificity to diagnose HPV-induced OPSCC [43].

2.6.2 HPV in situ hybridisation (ISH)

ISH has the peculiarity to allow direct view on DNA/RNA in tumour cells, thus a positive response has high specificity. Nevertheless, the pattern of positivity is distinguished into two forms and the technique is difficult and expensive too. The main con is the low sensitivity that changes in relation to the level of E6 and E7 expression [37].

2.6.3 HPV mRNA ISH (RNAscope)

E6/E7 mRNA ISH is an emergent technique easy to perform and with high specificity because this method allows the direct visualization of the RNA inside the cells. The available probes permit to identify various HPV subtypes. RNA ISH represents a good test with low inter-operator variability , high sensitivity and specificity [37].

2.6.4 Polymerase chain reaction (PCR)-based techniques

PCR is a very sensitive method that detects only a few copies of viral DNA in each sample, and it may use reverse transcriptase to amplify oncoproteins mRNA. Thus, mRNA RT-PCR is considered the

gold standard to detect the viral presence in tumours. The ideal condition to obtain the highest performance is the examination of fresh or frozen tissue, while in formalin-fixed and paraffin-embedded (FFPE) tissue this technique may fail because DNA and RNA are usually damaged.
RNA analysis is, unfortunately, quite complex and its application is often limited as only FFPE samples are available in the clinical setting [42].

2.6.5 HPV serology

L1 capsid proteins have the highest immunogenic activity but the presence of anti-L1 antibodies does not correlate with the presence of an HPV-driven tumour. By contrast, those against E6/E7 oncoproteins are heavily connected with oncogenesis [44]. Specifically, E6 seropositivity showed to be associated with a very increased risk to develop cancer and the presence of antibodies seems to begin very earlier than the tumour growth; this peculiarity could help in detecting sub-clinical HPV-driven neoplastic progression.
A recent review reported that considering each marker individually, HPV16 DNA positivity and p16INK4a were not significantly associated with a survival benefit, while seronegativity for the E6 and E7 oncoproteins resulted the strongest indicator of poor prognosis in oropharyngeal tumors [42]. The association between the HPV16 E6 seropositivity in pre-diagnostic phase and the subsequent development of an oropharyngeal cancer, the very low prevalence of E6 seropositivity in control subjects, make serological testing a valuable, clinically useful marker identifying HPV16-driven tumors. Moreover, seropositivity to HPV16 early proteins showed better prognostic significance respect to HPV-DNA detection and p16INK4a staining. Confirming this view, E6 seropositivity and/or seropositivity to more than two other early viral proteins have been shown to have a sensitivity and specificity of 95% and 98%, respectively, in detecting HPV-driven tumors [42].
Assays to quantify HPV-specific antibodies were based on Enzyme Linked Immuno-Sorbent Assays (ELISA); ELISA requires specialized laboratory and personnel, it is quite expensive, complex and time-consuming. Moreover, it requires pre-steps of sample processing, that can cause proteins denaturation and bioactivity modification.
Several authors investigated whether serum E6 and E7 antibody levels could potentially serve as a biomarker to detect patients with HPV+OPSCC or to identify patients with HPV+OPSCC whose disease recurred. In fact, the ratio of E7 antibody at disease recurrence compared with baseline was potentially a clinically significant measurement of disease status in HPV+OPSCC [45]. On the other hand, Hanna et al. [46] demonstrated the feasibility of measuring HPV16 E antibodies in saliva and

serum. E7 antibodies, in particular, are more detectable in saliva as compared with other E protein antibodies. Measuring E7 salivary antibody levels at various time points may have utility in understanding HPV clearance and should be explored for their ability to predict the risk of recurrence [46].

Nevertheless, there is no standard or routine HPV DNA testing for OPSCC; therefore, it is pivotal to develop a non-invasive and low-cost test [47]. The results of several studies support the idea of using salivary HPV DNA as a biomarker to monitor disease progression and tumour recurrence in OPC patients [48]. Previous studies demonstrated that the presence of HPV DNA in tumor tissues and plasma was significantly correlated with HPV DNA positivity in saliva samples collected from OPC patients [49].

Tang et al [49] supported the use of salivary HPV DNA as a non-invasive biomarker in OPC patients, and indicates that disease staging could be based on viral load in combination with an eighth edition staging system.

2.7 Biosensors

2.7.1 General features

Biosensors are devices that employ biological reactions for detecting analytes. Such devices combine a biological recognition element, interacting with the analyte, with a physical transducer that transforms the recognition into a quantitative electric signal. Common transducing elements, such as optical, electrochemical, or mass-sensitive devices, generate light, current or frequency signals, respectively [50,51].

A biosensor could be exemplified with three major components: a bio-element, a detecting element and a processor (Figure 5). The bio-element or bio-receptor should be sensitive and can be represented by enzymes, living cells or microorganisms, etc. which identifies the target analyte. The detecting element is the electrical interface that should monitor the changes in electric current and potential, impedance, optical intensity or electromagnetic radiations. In fact, due to the different signal detecting mechanisms, biosensors can be categorized into various types. The bio-element interacts with a signal transducer (the detecting element) which together transmit the changes/modifications of the analyte to a measurable signal [52].

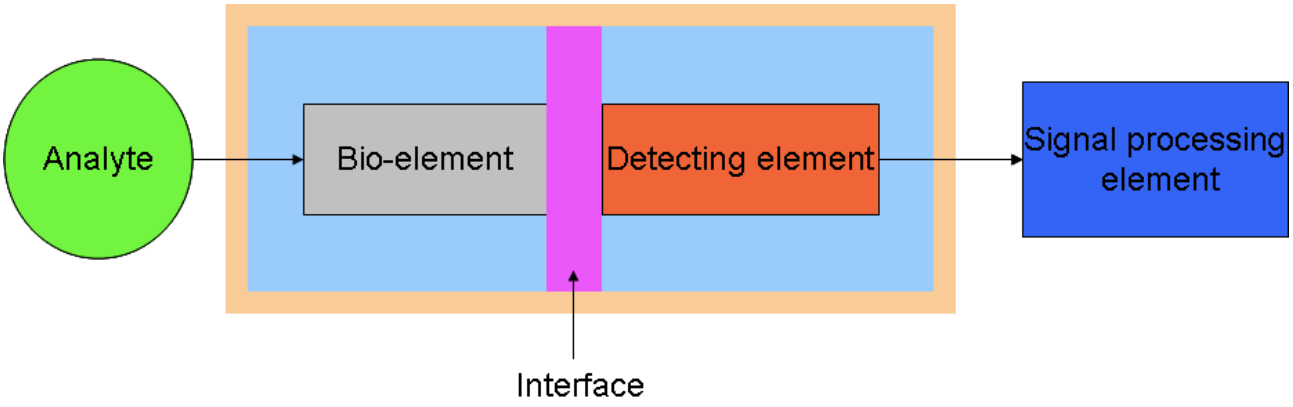

Figure 5. A schematic diagram representing the concept of a biosensor [52].

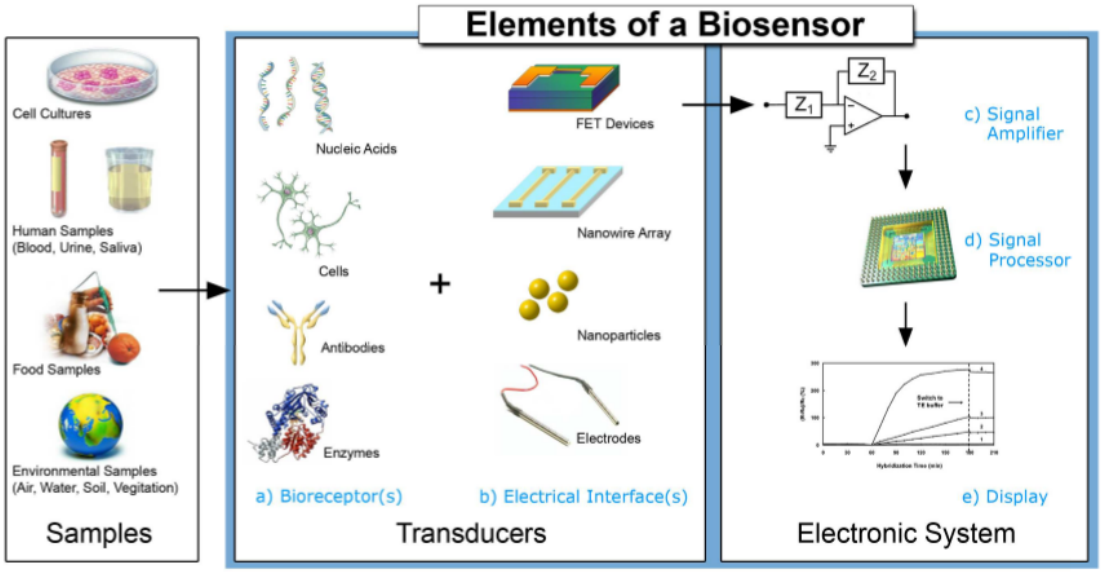

Figure 6. Schematic of a typical biosensor: a) biorecognition element that specifically bind to the analyte; b) an interface architecture where a specific biological event takes place and gives rise to a signal picked up by c) the transducer element; the transducer signal (which could be anything from the in-coupling angle of a laser beam to the current produced at an electrode) is converted to an electronic signal and amplified by a detector circuit using the appropriate reference and sent for processing by d) computer software to be converted to a meaningful physical parameter describing the process being investigated; finally, the resulting quantity has to be presented through e) an interface to the human operator [53].

2.7.2 The bioreceptor / The bio-element

The bioreceptor recognizes the analyte thus allowing a selective and specific response, limiting the interference with other elements of the sample. In electrochemical biosensors, the bioreceptor interacts with the analyte generating an electric signal proportionate to the analyte concentration. The biosensors can be classified into two groups based on how the process of recognition between analyte and bioreceptor works: catalytic and affinity biosensors [54].

Catalytic biosensors are also called metabolism biosensors based on the achievement of a steady-state concentration of a reaction. The progress of the biocatalysis is related to the concentration of the analyte, which can be measured by monitoring the growth of a product, the consumption of a reactant, or the inhibition of the reaction.

In affinity biosensors, indeed, the receptor molecule binds the analyte “irreversibly” and non-catalytically. The binding event between the target molecule and the bioreceptor, for instance an antibody, a nucleic acid, or a hormone receptor, is the origin of a physicochemical change that will be measured by the transducer. The peculiarity of this type of binding is the molecular recognition

property that exhibits molecular complementarity, through noncovalent bonding (hydrogen bonding, metal coordination, hydrophobic forces, van der Waals forces, π–π interactions, and/or electrostatic effects) [54]. The immunobiosensors belong to this category given that antigen-antibody complex formation requires a noncovalent binding between specific regions of both the antibody and the antigen.

An antigen is a molecule that triggers the immune response of an organism to produce an antibody, a glycoprotein produced by lymphocyte B cells which will specifically recognize the antigen that stimulated its production. Each antibody is a bivalent Y-shaped protein which has two identical Ag-binding sites located on each short arm. These regions confer complementarity toward the specific antigen and the boundary Ab-Ag is highly specific.

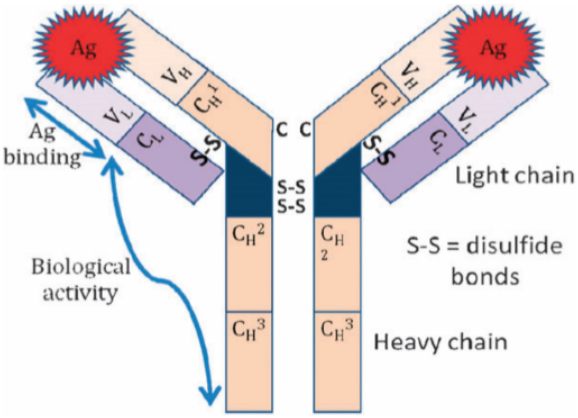

Figure 7. Y-shaped structure of an antibody and interaction between antibody and the antigen (Ag) in correspondace of the Variable region of the Heavy chain (VH) and Light chain (VL) [54].

2.7.3 Electrochemical Biosensors

The standard electrochemical biosensor consists of a matrix bound material fixed on an electrochemical transducer. Essentially, it is a surface modified electrical conductor for different electrochemical functions. This type of sensor targets those biological reactions that derive ionic production and consumption. This will cause the charge transfer across the double layer of the physio-chemical transducer that generates the measurable signal [55].

Electrochemical biosensors can be divided into amperometric, potentiometric and impedimetric biosensors.

Potentiometric biosensors are based on the ion sensitive field effect transistor (ISFET): the output signal is generated by the potential differences of oxidation/reduction reactions. The

electrochemical reaction generated ions are accumulated at the ion-sensitive membrane of the ISFET interface. When this potential is applied to the electrode, it modulates the current flow through the FET leading to a measurable potential of the detector [52].

Amperometric biosensors has a high sensitivity that allows detecting electroactive substances in biological samples. With a constant potential between the sensing and auxiliary electrode, the conversion of electroactive species takes place at the electrode. This will result in electron transfer, and the current is directly correlated to the bulk concentration of tested electroactive species [52].

In impedimetric systems, the chemical reactions that result in either ions production or consumption, will modify the conductivity of the solution; so, an impedimetric biosensor measures the solution's impedance (Z) change. Electrochemical Impedance (EI)-based biosensors can be combined with nanostructures and bio-probes thus increasing sensitivity, sensibility and reproducibility.

Furthermore, EI allows the monitoring of the addition of each layer on the sensing surface, including nano- and bio-materials, such as carbon nanotubes or graphene or metal nanoparticles, conducting or redox polymers, enzymes or antibodies.

The reactions are detected in proximity to the electrode surface, meaning that the type of the electrodes can influence the sensitivity and the specificity of the measurements: for this reason, the modification of the surface, called functionalization, is a crucial step.

DNA-based EIS biosensors with limit of detection in aptomolar range are reported in literature for the detection of small molecules as well as for HPV16 biomarkers [56]. However, a reliable HPV16 biosensor detecting anti-E6 and anti-E7 is not reported and, despite the body of research currently available, no POC biosensors are commercially available and can compete with more complex techniques in terms of sensitivity and limits of detection, to the best of our knowledge. Antibodies are quite big molecules (about 150.000 Dalton) therefore their presence on the electrode surface is detectable by measuring the variance of electrical capacity.

2.7.4 Biosensor performance

Depending on biosensor end use, the performance can be defined by different parameters [57]:

- sensitivity, that corresponds to the slope of the calibration curve, the change in the signal measured per unit of concentration of the analyte;
- limit of detection (LOD): is the lowest quantity of a substance that can be distinguished from the absence of that substance (a blank value) with a stated confidence level;

- dynamic range, the ratio between the largest and smallest values that a certain quantity can assume;
- selectivity, ability of the biosensor to specifically recognize a particular analyte or a group of analytes, influenced by the type of immobilization of the biological recognition system;
- reliability, is the overall consistency of a measure or of a system;
- Reproducibility is the closeness of the agreement between the results of measurements of the same measure and carried out with the same methodology described in the corresponding scientific evidence;
- resolution of a measurement system is the smallest yet to distinguish different in values. The specified resolution of an instrument has no relation to the accuracy of measurement;
- response time, is the total amount of time it takes to respond to a request for service as a function of the concentration of analyte;
- stability, ability to maintain its performance for a certain period of time;
- life cycle, the time during which the sensor works which is distinguishable between maximum storage time and maximum operating time.

3. AIM OF THE PROJECT

The project aims at developing a point-of-care (POC) device for the detection of Human Papilloma Virus (HPV)-driven oropharyngeal cancer, both for diagnostic and prognostic applications; the project will optimize an electrochemical impedance-based biosensor functionalized for the detection of HPV-specific antibodies as biomarker for cancer development.

The prognostic importance of HPV status arose from several clinical trials, such as the ECOG 2399 and the GORTEC 94-01 ones, which suggested that in HPV positive cancer a less aggressive treatment could be used to treat cancer efficiently.

Assays to quantify HPV-specific antibodies were based on Enzyme Linked Immuno-Sorbent Assays (ELISA); ELISA requires specialized laboratory and personnel, it is quite expensive, complex and time-consuming. Moreover, it requires pre-steps of sample processing, that can cause proteins denaturation and bioactivity modification.

An instantaneous self-test would be particularly useful to detect the presence of HPV antibodies in blood, both for diagnostic and prognostic purposes. A cheap test could really impact on developing countries in the context of cancer prevention.

A successful route to replace the immunoassay is the synthesis of the antigens that are expected to be complementary in size and affinity to the human anti-HPV antibodies. This system may bind the analytes, that are the antibodies we are looking for, in a similar way to that of natural interaction antigen-antibody. This work describes different type of antigens production (E7 and E6 oncoproteins), different types of the electrode surface functionalization and, finally, the analytical data on the performance of the device are reported. Recombinant protein production offers critical aspects, due to its complex structure and mutable spatial arrangement. A successful design should meet the exact conditions under which the native protein exists; on the other hand, considering that surface imprinting is a bottom-up approach, it should be considered the resembling nature's processes of building complex structures. Two main needs are required for a successful protein-based device for human antibody determination in POC: 1) the system should be disposable to allow a direct and easy handling of biological fluids in hospital; 2) it should allow the covalent link of the antibodies to the biosensing surface, to ensure that it remains there after its contact with liquid phase. The first requirements may be achieved by used the screen-printed-electrode (SPE) technology. The great progresses of this field originated a huge production of low-cost, reproducible and sensitive disposable electrodes. The second requirement may be fulfilled by selecting gold sur-

faces. Over the past decades [58] many biosensors have used self-assembled monolayers (SAMs) as a way to immobilize, in an ordered manner, organic molecules on gold surfaces [59]. This organic thin-film material layer may turn out a successful and highly controlled way to link the imprinting layer to the gold surface.

The resulting biosensor is evaluated by several electrochemical techniques and further applied to the analysis of biological samples.

Therefore, the project aims at developing a novel biosensor based on Au-SPE modified by self-assembly for the detection of HPV specific antibodies in POC applications. The resulting device is evaluated using the Electrochemical Impedance Spectroscopy (EIS) and further applied to the analysis of biological samples (the technology is described in the patent nr. MI2014A000146, Ulisse BioMed 2015).

The study is organized into three main parts:

1. development of a biosensor based on Au-SPE functionalized with SAM (4-ATP – MUA) SWCNTs and a commercial mixture of E7 peptides (PepMix) acting as the antigen to capture serum antibodies
2. the second part of the work was focused on the recombinant production of E6 oncoproteins and a different electrode functionalization.
3. the last part reported the analysis of biological samples.

4. MATERIALS AND METHODS

4.1 Human sera

Human sera were collected from volunteers aged between 25-35 years old both male and female that constitute the negative pool as control. Serum samples have been centrifuged to separate serum from hematic cells and then they were stored at -20° degrees to limit damages. Before each measurement, the samples were homogenized by gently shaking.

Commercial positive serum WHO (World Health Organization) is considered the international standard for HPV16 DNA in National Institute for Biological Standards and Control (WHO International Standard 05-134 HPV 16 antibodies; NIBSC code: 05/134 and it represents a pool of positive sera, was used as positive reference for the interpretation of the results [60,61].

Moreover, we collected a sample of blood from each patient affected by OPSCC who underwent a primary surgical treatment from January 2016 to June 2019. Patients were informed about the purpose of the study and gave their written consent (IRB: AULSS2/312.2017; amendment: Nr 624.2019). Twelve mL of whole blood were drawn for each 5 mL of serum or plasma needed; it was collected in an appropriate collection tube.

Then, it was centrifuged for at least 15 minutes at 2200-2500 RPM and the serum or plasma was pipetted into a clean plastic screw-cap vial. The sample was stored at -80°.

The table below summarizes the anamnestic data of enrolled patients.

CODE	SEX	AGE	TUMOUR SITE	TUMOUR STAGE (T)	LYMPHNODE STAGE (N)	HPV STATUS
TS_01	F	55	unknown primary	Tx	N2a	neg
TS_02	M	61	tonsil	T2	N2b	**HPV16**
TS_03	F	82	tonsil	T2	N1	**HPV16**
TS_04	M	70	unknown primary	Tx	N2b	neg
TS_05	M	69	tonsil	T3	N2a	neg
TS_06	M	65	base of tongue	T4a	N0	**HPV16**
TS_07	F	68	tonsil	T2	N1	**HPV16**
TS_08	M	85	unknown primary	Tx	N3b	neg
TS_09	F	82	tonsil pillar	T2	N0	neg
TS_10	F	74	base of tongue	T1	N0	neg
TS_11	F	67	tonsil	T1	N3b	neg
TS_12	M	74	unknown primary	Tx	N2b	neg
TS_13	M	79	tonsil	T3	N0	**HPV 16**
TS_14	M	70	base of tongue	T2	N0	**HPV16**
TS_15	F	78	tonsil	T2	N2b	**HPV 16**
TS_16	M	39	unknown primary	Tx	N2a	**HPV 16**
TS_17	M	61	soft palate	T3	N1	neg
TS_18	F	57	tonsil	T4a	N0	**HPV 16**
TS_19	M	73	base of tongue and tonsil	T2	N2b	**HPV 16**
TS_20	M	65	tonsil	T3	N0	**HPV 16**
TS_21	F	77	tonsil	T4a	N2b	**HPV 16**
TS_22	M	70	tonsil pillar	T2	N2a	**HPV 16**
TS_23	F	67	tonsil	T4a	N2c	**HPV 16**
TS_24	F	64	tonsil pillar	T1	N2b	neg
TS_25	F	84	tonsil pillar	T2	N2b	neg
TS_26	M	45	tonsil pillar	T2	N2b	neg
TS_27	M	87	soft palate	T1	N0	neg
TS_28	M	58	tonsil	T1	N0	neg

Table 3. Anamnestic data of enrolled patients. Tumour stage (T) and lymph node stage (N) established according TNM classification. Neg= HPV negative status.

The most common subsite was the tonsil (11 cases) followed by tonsil pillar (5), unknown primary tumour (5), base of the tongue (3) and 2 OPSCC localized in the soft palate; in 1 case both the base of the tongue and the tonsil were involved. The HPV status is routinely defined by pyrosequencing of the DNA extracted from the surgical specimen.

4.2 Antibodies, reagents and solutions

The following commercial primary antibodies were tested:

- HPV16 E7 Antibody ED17 sc-6981: IgG_1 mouse monoclonal antibody obtained with E7-HPV16 protein (Santa Cruz Biotechnology);
- HPV16 E7 Antibody C-20 sc-1587: IgG caprine polyclonal antibody obtained with C-terminal E7-HPV16 fragment (Santa Cruz Biotechnology);
- HPV16 E6 Antibody N-17 sc-15849: IgG caprine polyclonal antibody obtained with N-terminal E6-HPV16 fragment (Santa Cruz Biotechnology);
- HPV 18 E6 Antibody C-17 sc-365089: polyclonal caprine antibody obtained with C-terminal E6-HPV18 fragment (Santa Cruz Biotechnology).

The following reagents and solutions were prepared and used for the experiments:

- 95-98% pure sulfuric acid (H_2SO_4) - Sigma-Aldrich used for electrochemical cleaning
- 95% pure 11-mercaptoundecanoic acid (MUA) Sigma-Aldrich used to compose the SAM;
- 97% pure 4-aminothiophenol (4-ATP) -Sigma-Aldrich used together with MUA to compose a SAM;
- 99,9% ethanol (CH_3CH_2OH) -Merck is a solvent used to carry SAM formation;
- 99% pure 1-ethyl-3-(3-dimethylaminopropyl) carbodiimide hydrochloride (EDC) - Sigma-Aldrich activates carboxyl groups to conjugate to amino groups between SAM and pepmix.
- 98% pure N-hydroxy succinimide (NHS) - Sigma-Aldrich increases reaction efficiency or stabilize active intermediate.
- 99,8% pure morpholino ethane sulfonic acid (MES) is a buffer used in the reaction between SAM and pepmix;
- Phosphate-buffered saline (PBS) is a buffer solution. It is a water-based salt solution containing disodium hydrogen phosphate, sodium chloride and, in some formulations, potassium chloride and potassium dihydrogen phosphate. The buffer helps to maintain a constant pH to preserve pepmix stability.

- Each electrochemical procedure has been conducted with a specific mediator (a solution of $K_4Fe(CN)_6*3H_2O$ and $K_3Fe(CN)_6$ (Sigma-Aldrich).

4.3 Peptides and Proteins

We tested different antigens to functionalize the electrode surface: E7-PepMix; in house E7 recombinant oncoprotein purification; E6 oncoprotein production.

4.3.1 Pepmix

We decided to apply to biosensors PepMix™, commercial reagents traditionally used for the antigen-specific stimulation of T-cells. Overlapping peptides are arranged along the amino acid sequence of proteins of interest in such a way that T-cell stimulation is optimized while the chance of missing T-cell epitopes is minimized. The PepMix™ we used is a pool of 22 peptides derived from a peptide scan (15mers with 11 aa overlap) through Protein E7 (Swiss-Prot ID: P03129) of Human papillomavirus type 16 for T cell assays (Product Code: PM-HPV16-E7) [62]. This is a complete protein-spanning mixture of overlapping peptides (just called PepMix™) used to cover the electrode surface thus rendering specific the interaction with the analytes.

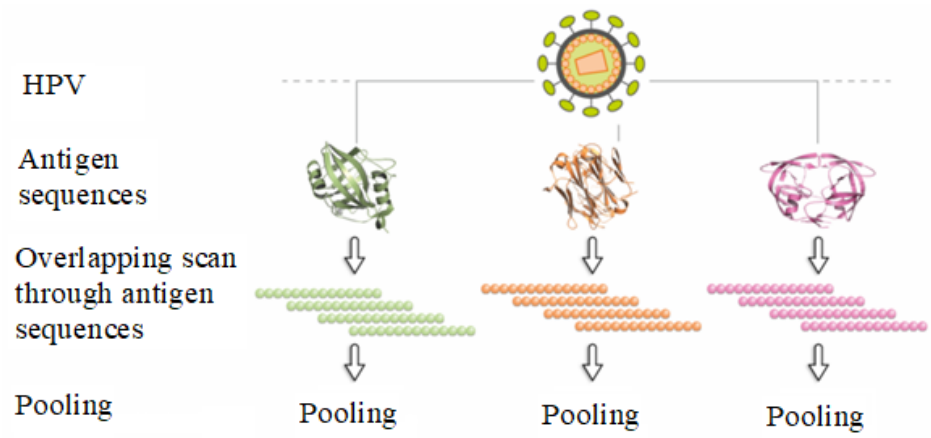

Figure 8. How the PepMix is produced; reworked version of an image from https://www.jpt.com/products/pepmix-peptide-pools/ [62].

In particular, we selected a E7-PepMix, a pool of 22 peptides derived from a peptide scan (15mers with 11 amino acids overlap) through Protein E7 (Uni-Prot ID: Q9QLP4) of Human papillomavirus type 06 for T cell assays [62].
E7 oncoprotein is made of 98 amino acids (11,022 Da) with the following sequence (Swiss-Prot ID: P03129):

```
                10                  20                  30                  40                  50
MHGDTPTLHE        YMLDLQPETT        DLYCYEQLND        SSEEEDEIDG        PAGQAEPDRA
                60                  70                  80                  90
HYNIVTFCCK        CDSTLRLCVQ        STHVDIRTLE        DLLMGTLGIV        CPICSQKP
```

4.3.2 HPV protein gene expression

In house purification of HPV recombinant proteins was based on a prokaryotic expression system (*Escherichia coli*). The sequences of the HPV16 E6 and E7 genes had been amplified from a HPV16+ patient and cloned into an inducible expression vector named pEQ30. The vector carries the polyhistidine affinity tag, for the subsequent chromatographic protein purification. Plasmids were kindly donated by Istituto Superiore di Sanità (ISS, Rome, Italy).

E7 protein production. E. coli strains JM109 and M15 harboring the pEQ30-E7 plasmid were grown in Luria-Bertani broth supplemented with ampicillin 100µg/ml, at 170 rpm 37°C. OD600 was measured with spectrophotometer to check bacterial growth and with OD600 = 0.6, induction was performed with 0.1mM of Isopropyl-p-D-thiogalactopyranoside added to the medium to induce E7 expression. After 4 hours of induction, the cells were pelleted and lysed to proceed with chromatographic purification using Nickel-nitrilotriacetic acid resin, under both native and denaturant conditions. The purified E7 oncoprotein was characterized by means of Sodium Dodecyl Sulphate - PolyAcrylamide Gel Electrophoresis, followed by Coomassie blue staining and Western blot analysis with a specific anti-E7 antibodies.

1. Remove cells from -80° freezer and Prelevare le cellule dal -80°C and let them thaw on ice for at least 15 minutes.

2. Prepare the number of tubes necessary for the transformation, plus a negative control (no plasmid transformation) and a positive one (transformation of one plasmid wiht known concentration)
3. In each tube, add 1ng-50ng of plasmid.
4. Distribute 100 µL of hte solution with *E.coli* XL1-Blue.
5. Briefly resuspend, then rest on ice for 30 minutes. Meanwhile, set up the thermostated bead bath system at 42°C for the heat shock.
6. Heat shock at 42°C for exactly 30 seconds, then immediately after taking the tube out of the water bath put it on ice.
7. Let stand on ice for 3 minutes. Do not mix.
8. Add 200µL of a rich medium (SOC, SOB, 2xTY) with no antibiotic and place in incubation with shaking 1 hour at 37°C
9. Warm selection LB-agar plates to 37°C.
10. Plate the cells marking the Petri dish
11. Overnight incubation at 37°C

E6 protein production. Several protocols were performed:

- E6 "Elisabetta" - 0.35 mg/mL 0.1% SDS in PBS, from bacterial strain JM109, denatured and stored at -20°C since 2016
- E6 "commercial" - 0.5 mg/mL in 12.5mM phosphate buffer, pH 8.8, 125Mm imidazol, 0.05% Tween 20 (purified from E.Coli under native condition) – protein
- E6 VT - 0.05 mg/mL in Hepes, pH 7.4, 5% glycerol, 50 mM NaCl, from yeast
- E6 VF - 0.2 mg/mL, 0.1% SDS, 0.02% Betaine in PBS, from bacterial strain JM109 (pools 17 and 21/05/18 mixed 1:1), denatured

4.4 Atomic Force Microscopy

The morphological analysis before and after HPV-oncoproteins depositions on the electrode surface was conducted by Atomic Force Microscopy (AFM) in tapping mode. This was done in collaboration with NanoInnovation Lab of Elettra Sincrotrone, Prof. Loredana Casalis, Trieste. A software was used to analyse the AFM images.

4.5 Enzyme Linked Immuno-Sorbent Assays (ELISA)

The Enzyme-Linked Immunosorbent Assay (ELISA) technique was adopted as reference standard technique. The indirect ELISA was chosen: it is a two-step ELISA which involves two binding process of primary antibody and labelled secondary antibody. The primary antibody is incubated with the antigen followed by the incubation with the secondary antibody [63].

The following commercial secondary antibodies have been used:

- Mouse Ascitic Liquid α-E6
- Polyclonal Ab - LS-C369152 (LifeSpan BioSciences) 4 mg/mL, IgG produced in Rabbit
- Secondary Ab α-Human - AB98535 (Abcam) 0.5 mg/mL
- Secondary Ab α-Rabbit - SC-2004 (SantaCruz) 0.4 mg/mL
- Secondary Ab α-Mouse - SC2005 (SantaCruz) 0.4 mg/mL

The ELISA was performed as control to quantify the interaction antibodies-pepmix. Briefly, polystyrene microwell plates (OptiPlate-96, White 96-well Microplate (PerkinElmer) or Black polystyrene Non-binding 96 well microplate (only for sera-preincubation) were coated with different proteins or pepmix in a coating buffer (100 µl/well); different coating buffer were tested in this study, such as carbonate buffer, pH 9.6, overnight at 4°C.

After incubation (that was performed in different conditions and temperatures), the coated wells were washed three times with 0.05% Tween in PBS (PBS-T, 200 ul/well) and left to block with a blocking buffer for at least 30 min at room temperature. Several blocking buffers have been tested such:

- 0.2% Casein: 100mg in 50mL of PBS-T (x2) - hard to dissolve, 8h at 40°C under stirring and then filtered
- 1% not fat dry milk (NFDM): 500mg in 50mL of PBS-T (x2) - filtered before use

- 1% goat serum (GS): 500µL in 50mL of PBS-T (x2)

Three Washing steps with PBS-T (200 ul/well) were performed. The primary antibodies, controls and serum samples were diluted in buffer and later incubated on the wells with different conditions and temperatures. Subsequently, the wells were washed three times with PBS-T and secondary antibody was added at proper dilutions. After additional washings with PBS-T, the kit SuperSignal ELISA Femto Maximum (ThermoFisher Scientific) was used according manufacturer's protocol for luminescence detection. Luminescence was measured using Envision Microplate Reader (Perkin Elmer) and the data were processed using excel Software.To optimize ELISA protocol, the following reagents have been tested:

- Bovine Serum Albumin (BSA)(Roche): it is a protein used to fill spaces not occupied by the primary antibody (blocking procedure) to avoid non-specific interactions with the secondary antibody;
- Triton™ X-100 (Sigma-Aldrich) it is a non-ionic surfactant and emulsifier useful in removing some non-specific binding of the secondary antibody; meanwhile, TWEEN 20 (Sigma-Aldrich) is used in the indirect ELISA to wash unbound antibody.

4.6 Electrochemical measurements

The electrochemical measurements, that is the voltammetry and the impedance spectroscopy, have been performed with the Potenziostat PalmSens3 connected with a special software "PSTrace 5.3" to measure the alternated current (AC) sinusoidal signal and to elaborate data.

The experiments were conducted with screen-printed electrodes Dropsens DRP-250AT.

The electrochemical cell consists of a working (4 mm diameter) electrode made of gold, a counter electrode that is made of platinum and a reference electrode made of silver (Ag); also electric contacts are made of silver. Both the electrode and the potentiostat are placed in a Faraday cage to minimize the electromagnetic field. The electrodes were connected to the potentiostat by means of specific connectors that act as interface between them.

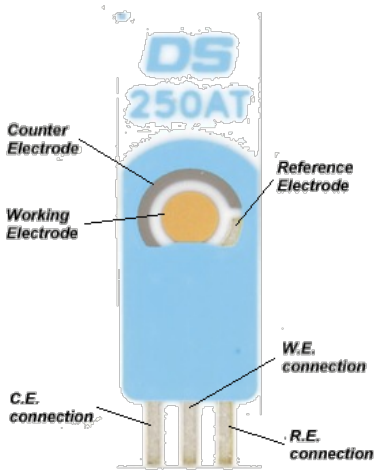

Figure 9. An image of a Dropsense screen-printed electrode. W.E.: working electrode; R.E.: Reference electrode; C.E.: Counter electrode. http://www.dropsens.com/en/screen_printed_electrodes_pag.html

Electrochemical analyses are done via cyclic voltammetry (CV) and electrical impedance spectroscopy (EIS) to characterize the electrochemical reversibility of the material, as well as its impedance at the electrode-solution interface; in particular, these techniques test the reversibility of electron transfer and impedance at the electrode-solution interface, respectively. In this study, we used the cyclic voltammetry to characterize the electrode surface and the electrochemical spectroscopy to detect the antibodies in human sera.

4.6.1 Cyclic voltammetry

The electrochemical properties related to the electroactive surface area are studied by cyclic voltammetry (CV). CV is used to understand and characterize the redox characteristics, stability, and effective surface area of an electrode for biosensing; such electrodes, modified with materials (the antigen in our case), function as a transducer to convert ions into measurable electrons.
CV is a useful electrochemical technique that permits to identify the changes regarding redox system mechanisms and transport properties of an electroactive species in solution. This technique represents the first step performed to characterize an electrode material for every type of application.
This method provides rapid information on the thermodynamic redox processes, on the kinetics of heterogeneous electron-transfer reactions, and on coupled chemical reactions or adsorption processes. Thus, this technique allows to evaluate the substances effects on the processes in the

solution. CV typically consists of a three-electrode setup of a working electrode (WE), a reference electrode (RE), and a counter electrode (CE). In CV, a potential applied to the WE is swept back and forth for a defined number of cycles over a given range of voltage and speed of voltage sweep. As the potential is scanned across a specified potential range, the resulting current at the WE is measured. The current generated is then plotted against potential to produce a CV graph that provides insights on the transducer material based on the anodic peak current (Ipa) from oxidation process and cathodic peak current (Ipc) from reduction process which occur on the WE. The potentials at which the peak currents occur are known as peak potentials (Ep). These peak potentials enable us to analyze the electrochemical reversibility of the reaction at the electrode surface by increasing the scan rates during experiments. The technique is preferably appropriate for a rapid search of redox couples present in a system, and once located a couple may be characterized by more careful analysis of the cyclic voltammogram. Usually, the potential is scanned back and forward linearly with time between two extreme values using a triangular potential waveform [64]. The most common method to determine the electroactive surface area is the ferro/ferricyanide redox couple method [65]. Ferro/ferricyanide redox system gives rise to a reversible redox system that involves one electron per molecule. Given the one electron involving and chemical reversibility of the redox system, the cyclic voltammetric analysis of the ferro/ferricyanide process envisaged the determination of the electroactive area of the electrodes through the apparent diffusion coefficient of this redox system on these electrodes, calculated based on the Randles–Sevcik equation:

$$I_{pf} = (2.69 \times 10^5) n^{3/2} A D^{1/2} C^* v^{1/2}$$

Thus, using cyclic voltammetry recorded at different scan rate in the presence of 4 mM $K3Fe(CN)_6$, the electrochemical behaviour of ferrocyanide system is studied after CV recording, which offers the opportunity to determine the characteristics of a cyclic voltammetric response originating from a reversible process. The reversibility of the system was estimated by the peak-to-peak separation. Another important parameter that is relates to the electrochemical reversibility of an electrode reaction is the peak current, and more specific, the ratio between the anodic peak current and the cathodic peak one, whose value is unity for a simple reversible couple.

The background current is given by the capacitive component of the electrical double layer and it is desired that this component to be minimized. However, it is well-known that the electrode characterized by the electrocatalytic activity has a high background current and low potential value

for the oxygen evolution, which denotes a narrow potential window. Though, this type of electrodes is very useful for the detection application especial for the hard oxidizable or reduction species.

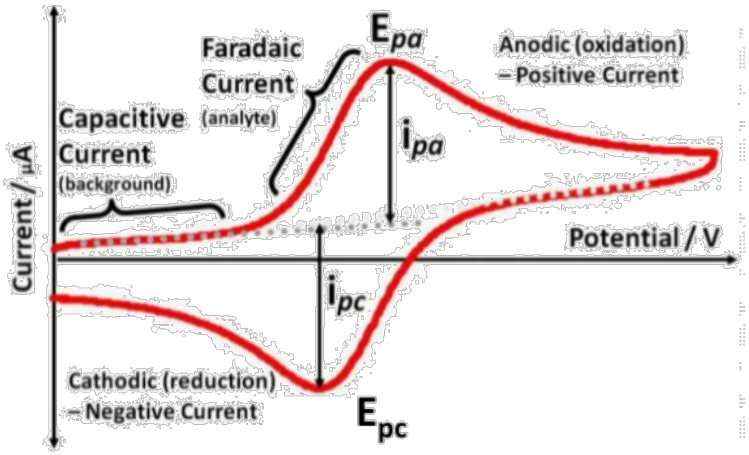

Figure 10. Typical cyclic voltammogram where i_{pa} and i_{pc} show the peak cathodic and anodic current respectively for reversible reaction. *https://www.slideshare.net/AfrinNirfa1/cyclic-voltammetry*

4.6.2 Electrochemical Impedance Spectroscopy (EIS)

EIS is an analytical tool to study the interfacial behavior occurring on the surface of an electrode. The impedance of an electrode at the electrode-solution interface is determined by applying a small alternating (AC) sinusoidal voltage (~10 mV peak-to-peak) perturbation and tracking the current output [66]. Since an AC is applied across the surface of the electrode, the voltage–current output will also be observed in a range of frequencies [67].

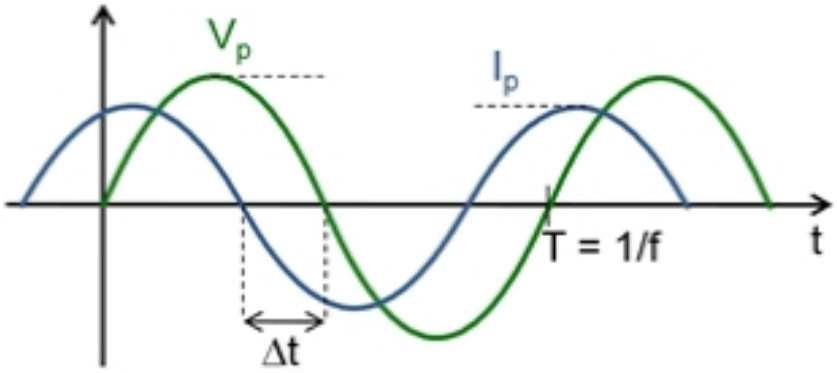

Figure 11. Schematic representation of the potential excitation and current response in the measurement setup.

A small sinusoidal variation is applied to the potential of the working electrode and the resulting current is analyzed in the frequency domain. The real and imaginary components of the impedance give information on the kinetic and mass transport properties of the cell, as well as on the surface properties through the double layer capacitance. EIS utilizes a small amplitude, alternating current (AC) signal to probe the impedance characteristics of a cell. The AC signal is scanned over a wide range of frequencies to generate an impedance spectrum for the electrochemical cell under test. EIS differs from direct current (DC) techniques in that it allows the study of capacitive, inductive, and diffusion processes taking place in the electrochemical cell.

Impedance is the tendency of a substance to oppose the passage of alternating current (AC) in a complex system, consisting of both resistors and capacitors. If the system is purely resistive, then the opposition to alternating current or direct current (DC) is simply the resistance of the circuit.

The experimental data can be represented in two ways, i.e., the Nyquist plot (where the real vs. imaginary impedance components are plotted) and the Bode plot (where the impedance and phase angle were plotted against frequency). The data obtained from experimental studies can be analyzed and evaluated using an equivalent circuit comprising a series of resistances and capacitances in parallel (Randles equivalent circuit) [68]. Note that the Nyquist plot will be preferred in this study because of the extensive information that can be obtained to understand the impedance at the electrode-solution interface, charge transfer resistance, and Warburg impedance.

A Bode plot (Figure 12) is a graphical representation of the frequency response of a linear time-invariant system (LTI) which consists of two graphs representing the amplitude (or modulus) and phase of the complex frequency response function respectively. The **Bode plot** is actually two plots in one. The abscissa is a logarithmic scale of the frequency and one ordinate is the logarithm of the impedance Z while the second ordinate is the phase shift Φ. The advantage of this plot is that all information is clearly visible. A capacitor in parallel to a resistor, which is an important circuit for electrochemical impedance spectroscopy, is visible in this spectrum as a peak in the phase shift. Single components can be easier understood.

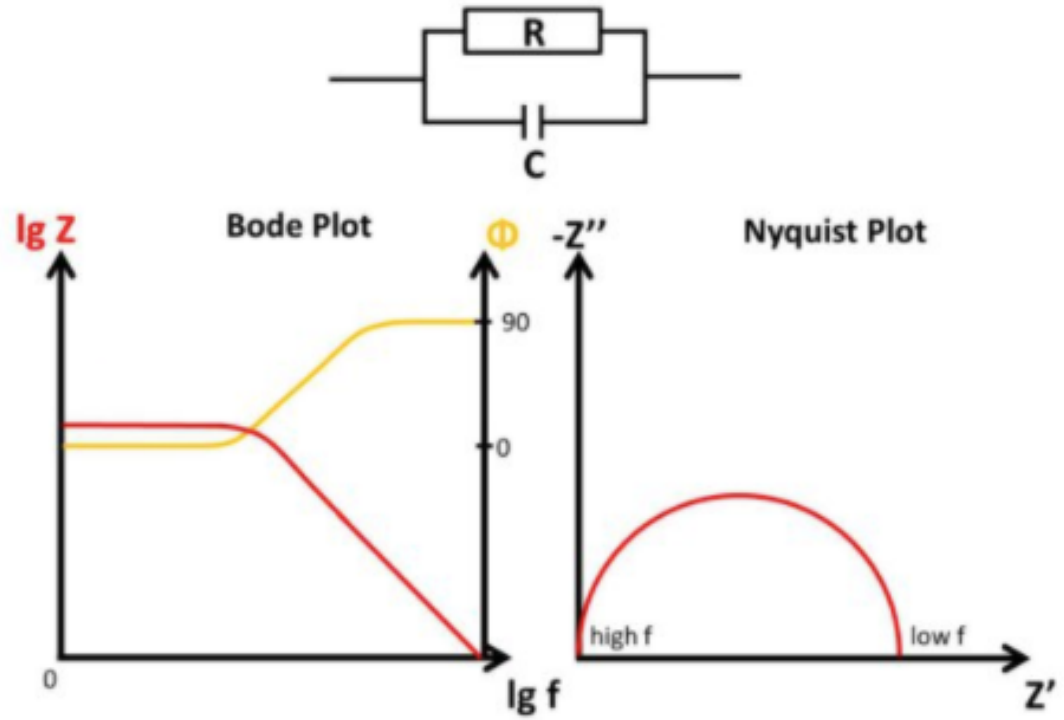

Figure 12. EIS of a parallel Resistor and Capacitor in a schematic Bode and Nyquist plot
Source: https://www.palmsenscorrosion.com/knowledgebase/bode-and-nyquist-plot/

The Nyquist plot is very sensitive to changes and for the most common circuits some parameters can be read directly from the plot. To get a Nyquist plot the negative imaginary impedance –Z'' is plotted versus the real part of the impedance Z'. Contrary to the polar representation, or Nyquist diagram, the representation of the module and phase of the transfer function does not take place on a single Cartesian plane, but in two distinct ones which both have abscissa, as an independent variable, the frequency or the pulsation and ordinate precisely the modulus of the amplitude usually expressed in decibels or the phase expressed in degrees or radians.

This circuit is already quite close to a real system. The capacitor represents the electrochemical double layer $C_{dl,}$ which can only store charge. The resistor represents the charge transfer resistance Rct. This is the resistance for the electron to change the phase, e.g. from the electrode into the solution or to be more precise to a species solved in the solution. This happens during every electrochemical reaction. These are two ways for current to pass through the electrode-solution interface. All the current should pass through the solution, which acts as an Ohmic resistor Rsol. The resulting circuit is seen in Figure 13 and is called the simplified Randles circuit.

4.6.3 Warburg impedance

It was observed that some effects occur in EIS that can't be modelled with classic electronic components, so new components were introduced. One of them is the Warburg impedance. The Randles circuit is quite close to an electrochemical experiment. As mentioned before, the solution resistance R_{sol} is the serial resistor. All current needs to go through the solution.

Up to here the expected EIS would be a semi-circle just as for the simplified Randles circuit. If a free diffusing species is converted at the electrode, this behavior isn't observed. At low frequencies oxidizing or reducing potentials are hold long enough that depletion of the species in front of the electrode becomes relevant. The depletion of species in front of electrodes is well understood and described by the Cottrell equation. During an EIS measurement this is measured as an increase in impedance. This increase is represented by the Warburg Impedance W, which is a virtual electronic component only used to make equivalent circuits for electrochemical experiments. The Warburg element's impedance is calculated by Cottrell equation:

$$Z_W = \frac{\sigma}{\sqrt{2\pi f}} - j\frac{\sigma}{\sqrt{2\pi f}}$$

Where Z_W is the impedance of the Warburg element and σ is the Warburg coefficient also known as A_W. It has the unit $\Omega/s^{½}$ and can be extracted from measurement data or it can be calculated according to

$$\sigma = \frac{RT}{Az^2F^2\sqrt{2}}\left(\frac{1}{\sqrt{D_O c_O^b}} + \frac{1}{\sqrt{D_R c_R^b}}\right)$$

Where R and F are the Gas and Faraday constant, D is the diffusion coefficient and c^b the concentration of the species in the bulk. The indices O and R indicate the oxidized and reduced species.

The Warburg Impedance is visible in the Nyquist plot as a straight line with a 45 ° angle to the abscissa. As mentioned before the depletion has a significant effect on the impedance at lower frequencies. When it becomes visible depends on the double layer capacitance. A schematic representation of a full electrochemical system's EIS is shown in Figure 13.

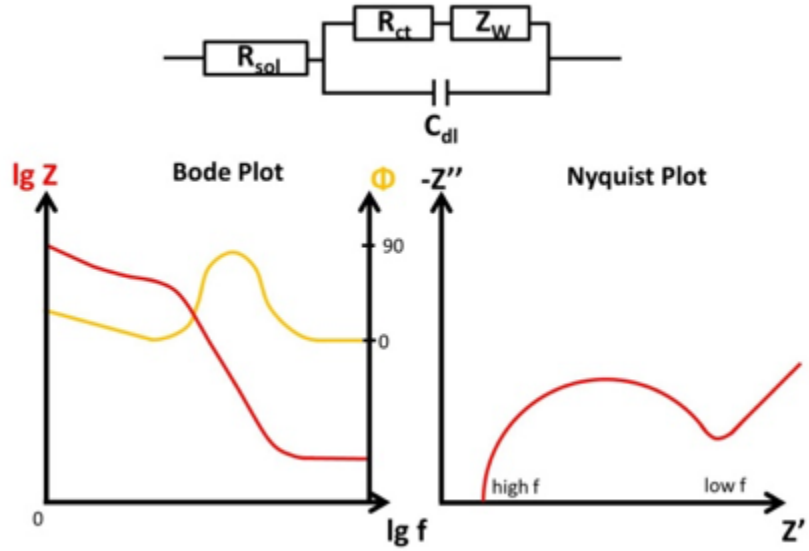

Figure 13. EIS of a Randles circuit including a Warburg element in a schematic Bode and Nyquist plot.

As mentioned before the Randles circuit contains a free diffusing species. This is typical for analytical electrochemistry, but does not have to be true for corrosion experiments. An example where this equivalent circuit works quite nice is a non-porous electrode (e.g. platinum disc electrode) and a reversible redox couple in solution (e.g. ferrocyanide and ferricyanide). Two examples are shown in Figure 14.

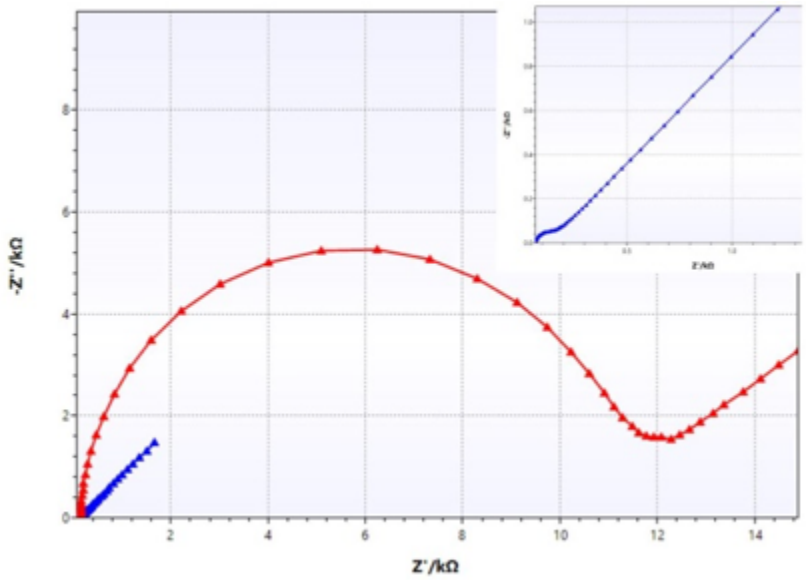

Figure 14. EIS of a Pt disc electrode (blue) and an IS-1 SPE (red curve) with a carbon ink working electrode in K3[Fe(CN)6] + K4[Fe(CN)6] solution; Insert: Zoom in on blue curve.
The platinum electrode (blue curve) has a very low charge transfer resistance, leading to a dominance of the Warburg impedance at very low resistances, while the carbon electrode by ItalSens (red curve) shows a significant higher charge transfer resistance, leading to the expected semi-circle.

Source: http://www.abnova.com/support/resources.asp?switchfunctionid={70196CA1-59B1-40D0-8394-19F533EB108F

4.7 Electrode preparation

4.7.1. Electrochemical cleaning of Dropsens SPEs

Before EIS, electrochemical preparation of the electrode was performed as following: cleaning is achieved through the combination of a chemical process with sulfuric acid and electrochemical with cyclic voltammetry [69]. The first step consists in deposing, under a chemical hood, a drop of sulfuric acid (H_2SO_4) 0,5M to entirely cover the working electrode (Dropsens DRP-250AT). The deposition takes place in 4 hours at least, after that the drop is removed from the working electrode and 10 cycles of voltammetry with 1 drop of H_2SO_4 0,5M are performed.

In the 10 cycles of CV, for the electrochemical cleaning of the electrodes, a potential range is applied ranging from 0V to + 1.25V with a speed of 100 mV / s [70].

After this process, the electrode is submerged in the 90mm Petri dish containing deionized H_2O, in order to completely remove the traces of H_2SO_4.

4.7.2. SAM deposition

After the cleaning of the electrode, we proceed with the formation of the self-assembled monolayer (SAM) on the working electrode.

Self-assembled monolayers (SAMs) form by the spontaneous adsorption of amphiphilic adsorbates onto an appropriate substrate. The initial driving force for the assembly is the chemical affinity between the adsorbates and the substrate. We tested different molecules and for each component the reaction is the same and leads to the formation of a covalent gold-sulfur bond (Au-S) [71].

SAM deposition happens by immersion in the 90mm Petri dishes, in which the cleaned electrodes are placed. The electrodes are submerged in a solution made of 10mL of pure EtOH and 10mM of SAM.

Once the electrodes are immersed in the solution, they are stored at 4 ° C for at least 12 hours/24 hours.

After that, the electrodes are submerged in a solution of pure ethanol, so as to allow the removal of the excess SAM. Finally, to remove the possible traces of EtOH, an immersion washing in deionized H_2O is carried out.

At this point, to demonstrate the successful formation of the SAM, measures are taken at room temperature both with the CV and with EIS. Both measurements require a solution of $K_3Fe(CN)_6$ 5mM in H_2O.

In CV, a potential range from -0.5V to + 0.6V and a speed of 100 mV / s is applied.

On the other hand, in EIS, a base potential of 0.0V vs open circuit potential (OPC) is applied, a maximum and a minimum frequency of 2000.0 Hz and 0.25 Hz respectively with a number of frequencies of 40 = 10 / dec.

The impedance analysis is carried out at time-zero, that is when the drop is deposited on the electrode surface, and with regular intervals of 5 minutes up to 15 minutes, in which it is possible to confirm the stability of the measurement

We tested the following SAMs:

- 4-aminothiophenole (4-ATP);
- mercaptoundecanoic acid (MUA);
- hybrid coating made of 11-Mercaptoundecanoic acid (MUA) and Triethylene glycol mono-11-mercaptoundecyl ether (TOEG3).

4.7.3 Electrode coating (functionalization)

Once that the Au-S covalent bond has been formed, electrode was then coated with the antigen thus allowing the formation of covalent bonds with SAMs. Finally, the redox couple $Fe(CN)_6^{3-/4-}$ was used to test the electrode and the signal, detected as charge-transfer resistance (R_{CT}) change, was measured before and after adding a solution containing anti-E7 antibodies in presence of 1% serum.

Protocol of electrode functionalization:

1. SAM 30% 11-Mercaptoundecanoic acid (MUA) - 70% Triethylene glycol mono-11-mercaptoundecyl ether (TOEG3) - 14h, dark, 4°C:
    - 225µL of 2mM MUA + 3.5mL of 300µM TOEG3 + 6.3mL of EtOH = 10mL solution, total concentration 150Mm

2. Activation of -COOH with EDC-NHS - 50µL/electrode, 30', rt
    - 200mM EDC (solution A): 16.8mg di EDC in 438µL di 10mM MES pH 6.5
    - 50mM NHS (solution B): 4.7mg di NHS in 817µL di 10mM MES pH 6.5
    - Mix solution A and solution B (ratio 1:1) immediately before the use to obtain the solution 100mM EDC, 25mM NHS, 10mM MES, pH 6.5 to be deposited on the SPEs
3. E6 binding - 40µL/electrode of 10ng/µL E6, 1h, dark, 37°C
   7µL of 0.27mg/mL E6 + 182µL of 10mM MES, pH 6.5
4. Blocking with 100mM Glycine methyl ester - 1h, rt, dark 10.9 mg in 867µL of PBS
5. PBS, 4°C, dark

*washing with water and dry the surface (to let the deposition of the drop) after each step.

4.7.4 EIS measurement

Measurement performed in 50µL of 5mM $Fe(CN)_6^{3-/4-}$ in PBS (RE, WE and CE must be completely covered by the solution) with the following parameters:

- Waiting time (between measurements): 240s
- OCP measuring time: 60s
- First additions: 50µL with doubled concentration to have the right concentration in the measuring solution, with 5mM $Fe(CN)_6^{3-/4-}$ in PBS (eg add 2% human serum to have 1% human serum in the measuring solution)
- Second additions: 100µL (or 50µL after removing 50µL from the measuring solution) with doubled concentration as above

5. RESULTS:

5.1 Verification of the electrochemical cleaning

The aim of the study was to develop a sensor able to detect antibodies in blood serum and to evaluate the potential use of this system for the detection of biomarkers in the early diagnosis of OPSCC. In fact, the presence of anti - E6 and E7 antibodies correlate with the prognosis of this pathology [31]. It was decided to operate with an electrochemical biosensor based on the EIS.

For this project, we selected a gold screen-printed electrode (Au-SPE) (DropSens DROPSENS (DRP-C220AT); first of all, it was important to perform an electrochemical cleaning with H_2SO_4 in cyclic voltammetry.

This type of electrodes is disposable and has a low production cost.

The graph in Figure 15 represents the first ten cycles of cyclic voltammetry; it is possible to see that the Au-reduction peak increased while the peaks of other volatile organic substances decreased, meaning that their depositions were superficial.

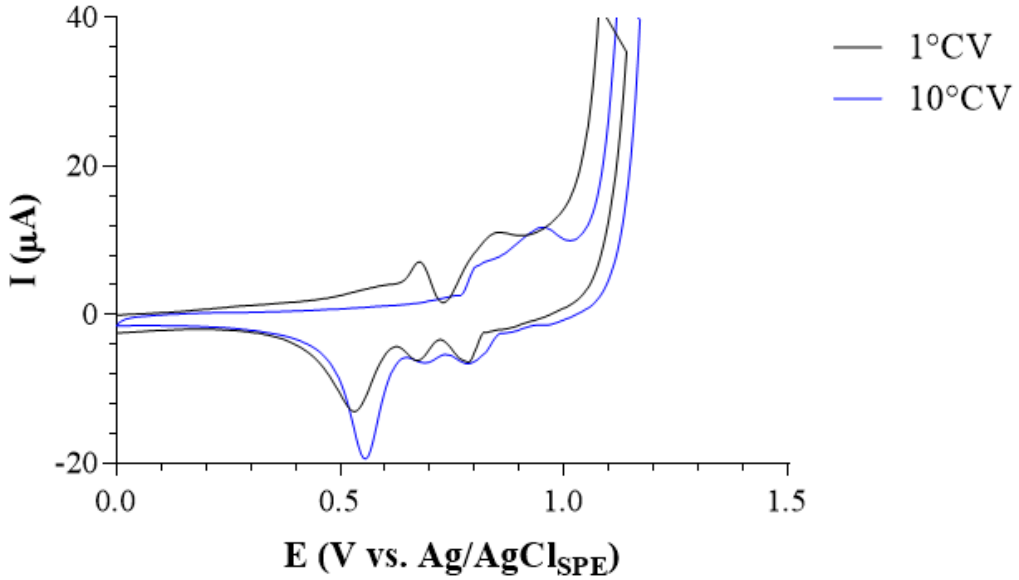

Figure 15. Voltammetry for electrochemical cleaning. The figure shows the voltammograms of the first and tenth cyclic voltammetry obtained with H_2SO_4 0.5M solution deposited on the Au-SPE surface. In the voltammogram, the current (I) is observed on the ordinate axis and it is expressed in microampere (µA), instead, on the abscissa axis, the potential (E) expressed in volts (V).CV was conducted with a range of potentials ranging from 0V to + 1.25V and at a scan speed of 100mV / s at room temperature.

The EIS was used to evaluate the features of the Au-SPE electrodes before and after the cleaning process and confirm that the electrode cleaning was successful (Figure 16).

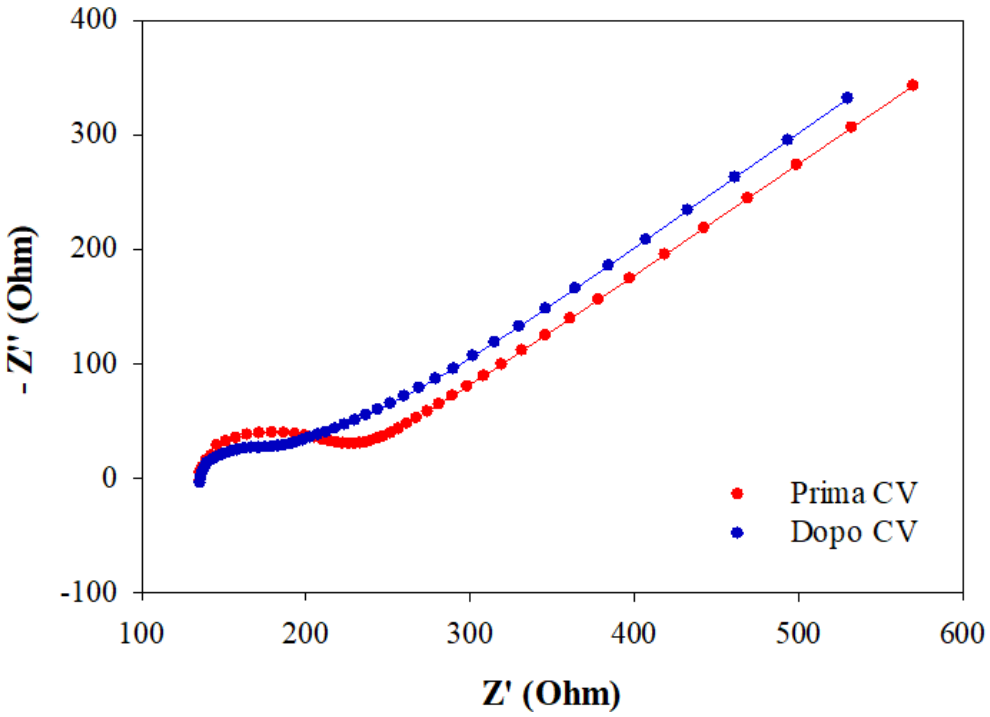

Figure 16. EIS analysis relating to the Au-SPE cleaning process. The figure shows the Nyquist plot of Au-SPE before cleaning (red dots), Au-SPE after cleaning (blue dots) with the respective fittings. The imaginary part is plotted on the axis of the ordinate –Z'' (Ohm), and abscissa represents the real axis Z'(Ohm). The analysis has been performed with a solution of $K_3[Fe(CN)_6]$ 5mM in H_2O at room temperature, with a basal potential 0.0V vs OPC, a maximum and minimum frequency of 2000.0Hz and 0.25Hz respectively with a number of frequencies of 40 = 10 / dec.

Graphically, it is observed that the clean electrode has a charge transfer resistance value, lower than the initial situation; this demonstrates the successful removal of volatile organic compounds. EIS measurements allow to analyze the electrochemical system in terms of equivalent electrical circuit. In this case, the circuit model (Figure 17), used to describe the system, is composed of the resistance of the solution (RS); by polarization resistance (RP); from the impedance of Warburg (W) and from the constant phase element (Q).

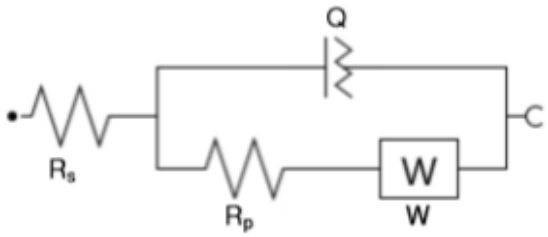

Figure 17. Equivalent electrical circuit. R_S =Resistance of the solution; R_P =polarization resistance; W = impedance of Warburg. https://www.researchgate.net/figure/263720227_fig1_Figure-4-Scheme2-Modified-Randles-Ershler-equivalent-circuit-with-constant-phase

5.2 Electrochemical characterization of the different SAMs

The SAM formation process is a fundamental phase to fix the bioreceptor on the gold surface, which is allowed thanks to the functionalization of the working electrode with molecules characterized by:

- a thiol group (-SH), able to react with the noble metal Au and allow the formation of the covalent bond Au-S;
- a carboxylic group (-COOH) or an amino group (-NH_2), that reacts with the antigen.

SAM analyses were carried out with the electrochemical techniques of CV and EIS.

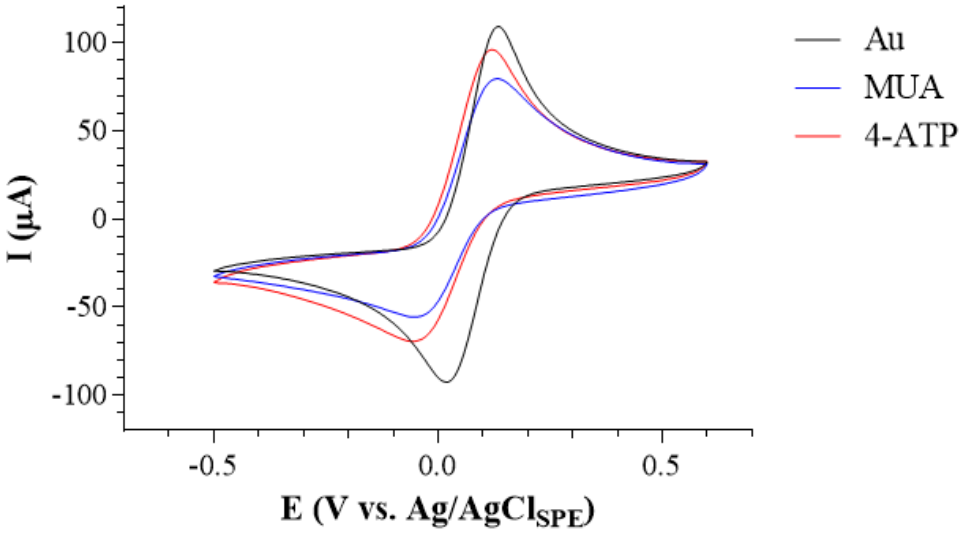

Figure 18. Voltammetry for the SAMs. The figure shows the voltammograms of the Au-SPE (black line), MUA (blue line) and 4-ATP (red line), obtained with a solution of $K_3[Fe(CN)_6]$ 5mM in H_2O. In the voltammogram, the current (I) is observed on the ordinate axis and it is expressed in microampere (µA), instead, on the abscissa axis, the potential (E) expressed in volts (V). CV was conducted with a range of potentials ranging from 0V to + 1.25V and at a scan speed of 100mV / s at room temperature.

In Figure 18 the voltammograms, obtained with the different peak potential values, show that changes on the working electrode can affect the kinetics of the redox reaction of the couple $Fe(CN)_6^{4-}/Fe(CN)_6^{3-}$.

The value of the potential, at which the oxidation or reduction of a chemical compound is observed, is typical of the redox species involved in the reaction; it is influenced by the nature of the support, with which the redox species exchange electrons.

Initially, the characteristics of the electrodes with the SAMs of MUA and 4-ATP compared to the Au-SPE electrode, illustrated in Figure 19, were assessed.

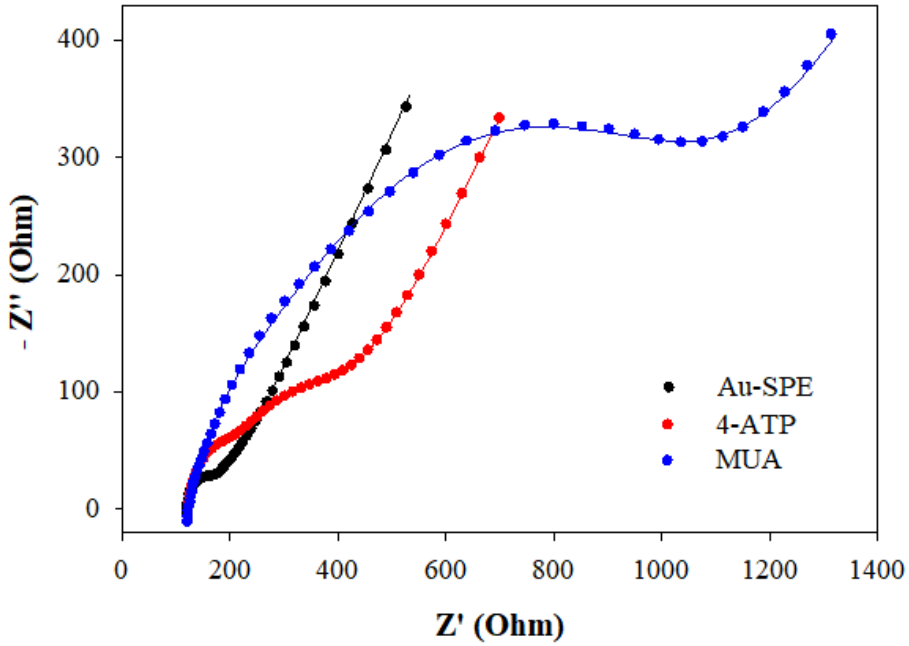

Figure 19. Au-SPE and SAM EIS analysis. The figure shows the Nyquist plot regarding Au-SPE (black dots), 4-ATP (red dots) e MUA (blue dots with relative fitting. The imaginary part is plotted on the axis of the ordinate –Z'' (Ohm), and abscissa represents the real axis Z'(Ohm). The analysis has been performed with a solution of $K_3[Fe(CN)_6]$ 5mM in H_2O at room temperature, with a basal potential 0.0V vs OPC, a maximum and minimum frequency of 2000.0Hz and 0.25Hz respectively with a number of frequencies of 40 = 10.

The Nyquist plot shows that the presence of SAMs on the electrode surface lead to an increase in charge transfer resistance. Moreover, the resistance of the Au-SPE is lower than that of the two SAMs, demonstrating that the formation of the monolayer occurred and the resistance to charge transfer increased.

5.3 PepMix analysis

To develop the biosensor, two different techniques have been followed. Since the precise epitope recognized by the human antibodies anti-E6 and -E7 remains still unknown, a mixture of peptides

derived from HPV proteins (Pepmix) and whole recombinant proteins have been used both as recognition and bonding method. Pepmix has the advantage to be cheap, has a high degree of purity due to it is synthetized, so it is also stable. Among cons, we underline that Pepmix corresponds only to linear epitopes so antibodies that recognize conformational epitopes are lost.

On the other hand, recombinant proteins allow to recognize antibodies that bond conformational epitopes; nevertheless, the production is not easy, particularly in HPV due to accentuate instability of the structure.

We chose 4-ATP because it presented a lower charge transfer resistance that MUA and the bond between pepmix E7 and the SAM of 4-ATP was verified with the EIS technique.

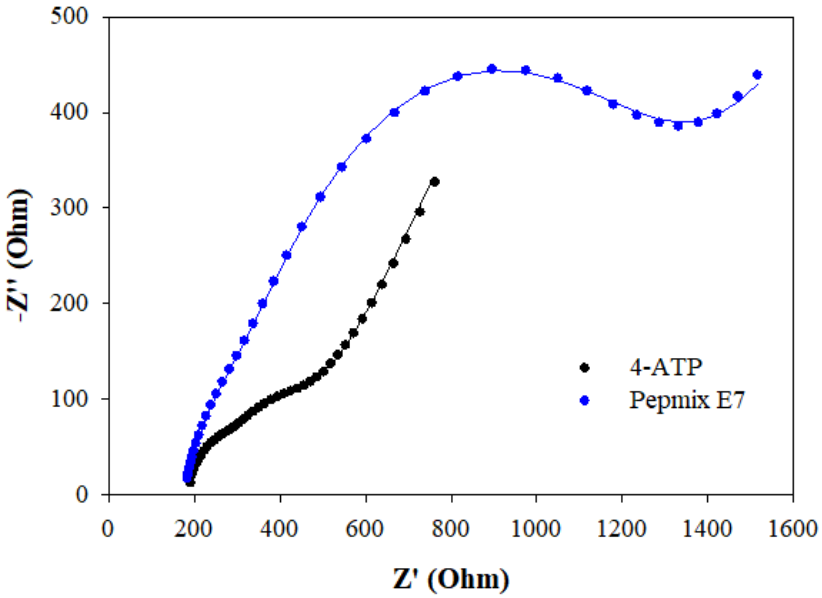

Figure 20. E7 pepmix immobilization on SAM of 4-ATP. The Figure reported the Nyquist plot regarding 4-ATP (black dots) and 200ng/15µL E7 pepmix(blue dots with relative fitting. The imaginary part is plotted on the axis of the ordinate –Z'' (Ohm), and abscissa represents the real axis Z'(Ohm). The analysis has been performed with a solution of $K_3[Fe(CN)_6]$ 5mM in H_2O at room temperature, with a basal potential 0.0V vs OPC, a maximum and minimum frequency of 2000.0Hz and 0.25Hz respectively with a number of frequencies of 40 = 10

With this experiment, we observed that E7 Pepmix had a greater resistance compared to only SAM, meaning that implies that the bioreceptor has been immobilized on the gold surface.

Then, we conducted the impedimetric analysis using commercial antibody to check the affinity with the pepmix.

We chose the polyclonal goat antibody because in ELISA it gave a greater luminescence signal compared to monoclonal mouse antibody, probably because it can recognize more epitopes of the pepmix E7.

From EIS experiments we observed that the negative signal, (that is the negative serum diluted to 1%), is higher than the signals obtained with the addition of 27nM anti-E7 antibody: this means that the system does not recognize the bond antibody-antigen.

We checked in ELISA and we noted that the negative serum had a lower background compared to signal obtained in presence of polyclonal antibodies.

This result showed that the reaction antigen-antibody happened, but it is not detectable by EIS: the signal produced by serum is much higher than those registered in presence of the antibody, this fact limits the detection.

Analysis	**<Counts>**
1% negative serum	<34006 ± 638>
1% negative serum + 27nM Anti-E7 Antibody (mouse)	<56802 ± 3242>
1% negative serum + 27nM Anti-E7 Antibody (goat)	<217604 ± 18148>

We reported below the Nyquist plot that shows a higher resistance with the antibody compared to the only pepmix, this shows that the bond antibody-pepmix happens without serum.

As shown in Nyquist plot reported in figure 21, we noted a higher resistance in presence of antibody in comparison to E7 pepmix alone: this proves the bind between antibody and E7 pepmix without serum.

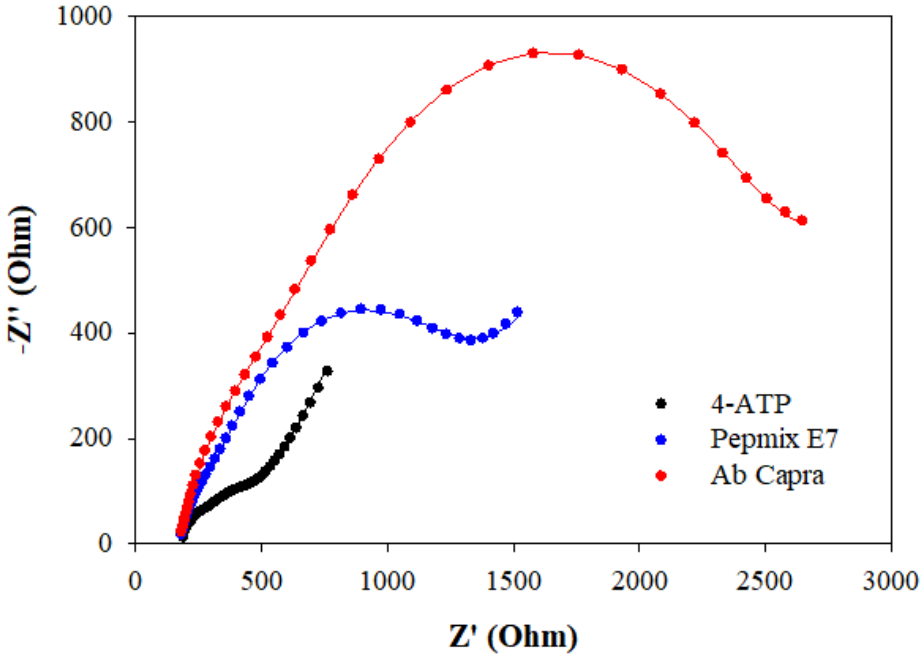

Figure 21. Interaction between E7 pepmix and anti-E7 HPV16 antibody with no serum. In the figure The Figure reported the Nyquist plot regarding 4-ATP (black dots) and 200ng/15µL E7 pepmix (blue dots with relative fitting. The imaginary part is plotted on the axis of the ordinate –Z'' (Ohm), and abscissa represents the real axis Z'(Ohm). The analysis has been performed with a solution of $K_3[Fe(CN)_6]$ 5mM in H_2O at room temperature, with a basal potential 0.0V vs OPC, a maximum and minimum frequency of 2000.0Hz and 0.25Hz respectively with a number of frequencies of 40 = 10

As a final experimental test to assess PepMix E7, indirect ELISA was performed with negative sera in comparison with commercial serum as positive control (WHO). This experiment was conducted in order to confirm whether the detection in serum of anti-E7 antibodies using pepmix is possible. Observing the Figure 22 below, the background signal in ELISA is changing among different negative sera ranging between 1,6 x 10^5 - 3,01 x 10^5 RLU (normalized value for E7 pepmix); moreover, we noted the WHO serum signal is included in the negative sera's range. The WHO serum is a pool of human sera belonging to patients affected by HPV-16 thus containing polyclonal antibodies that have not been characterized for titer and affinity towards oncoproteins E6 and E7. Therefore, the absence of signal in ELISA might be due to the lack of antibodies anti-E7 or to a failed recognition of pepmix E7, as short synthetic peptides.

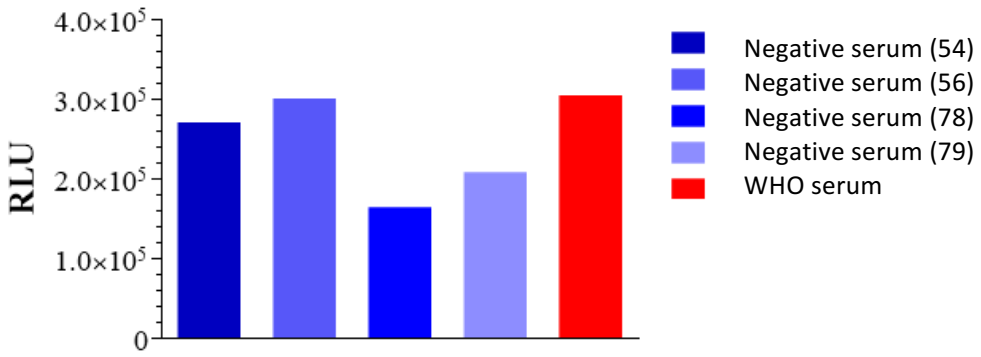

Figure 22. Interaction between E7 pepmix E7 with negative serum and WHO serum. The graph reports different negative sera and WHO serum normalized E7 pepmix (RLU negative or WHO serum – RLU E7pepmix). Ordinate axis reports the Relative Light Unit (RLU). Data are obtained with indirect ELISA on plate with Femto kit ELISA (Luminolo e H_2O_2 1:1).

In conclusion, the results obtained testing E7 pepmix showed that:

1. EIS with antibodies was not significant in presence of serum
2. E7 pepmix was not recognized by antibodies that react against WHO positive control.

This discouraged us to pursuing experiments with E7 pepmix and we decided to focus on whole proteins.

Moreover, the impedance measurements carried out highlight the importance of using the PBS in the measurement solution as a transport ion, otherwise the addition of the antibody (that is dissolved in PBS) changes the solution concentration with the consequent decrease in resistance, thus distorting the measurements.

5.4 RECOMBINANT E7 PROTEIN ANALYSIS

Since E7 pepmix was not able to provide a clear signal of detection even in the traditional method ELISA, we decided to focus on whole recombinant proteins, in particular HPV16 E7 and E6.

E7 recombinant oncoprotein was obtained from *E.coli* and it demonstrated sufficient stability. The purified E7 oncoprotein was characterized by means of Sodium Dodecyl Sulphate - Polyacrylamide Gel Electrophoresis, followed by Coomassie blue staining and Western blot analysis with a specific anti-E7 antibodies. Preliminary results showed that recombinant protein purification under denaturant conditions gave a better yield than native protein purification, however the latter allowed to obtain fully folded proteins. This protein was used to coat the electrode surface and we tested the ability to detect anti-E7 polyclonal antibody diluted in a 1% serum solution.

The figure below represents the impedance measurement of the electrode. The black line corresponds to the impedance in presence of the antibody that is higher compared to signal

obtained with only the serum (red line); the blue line represents the background which remains stable.

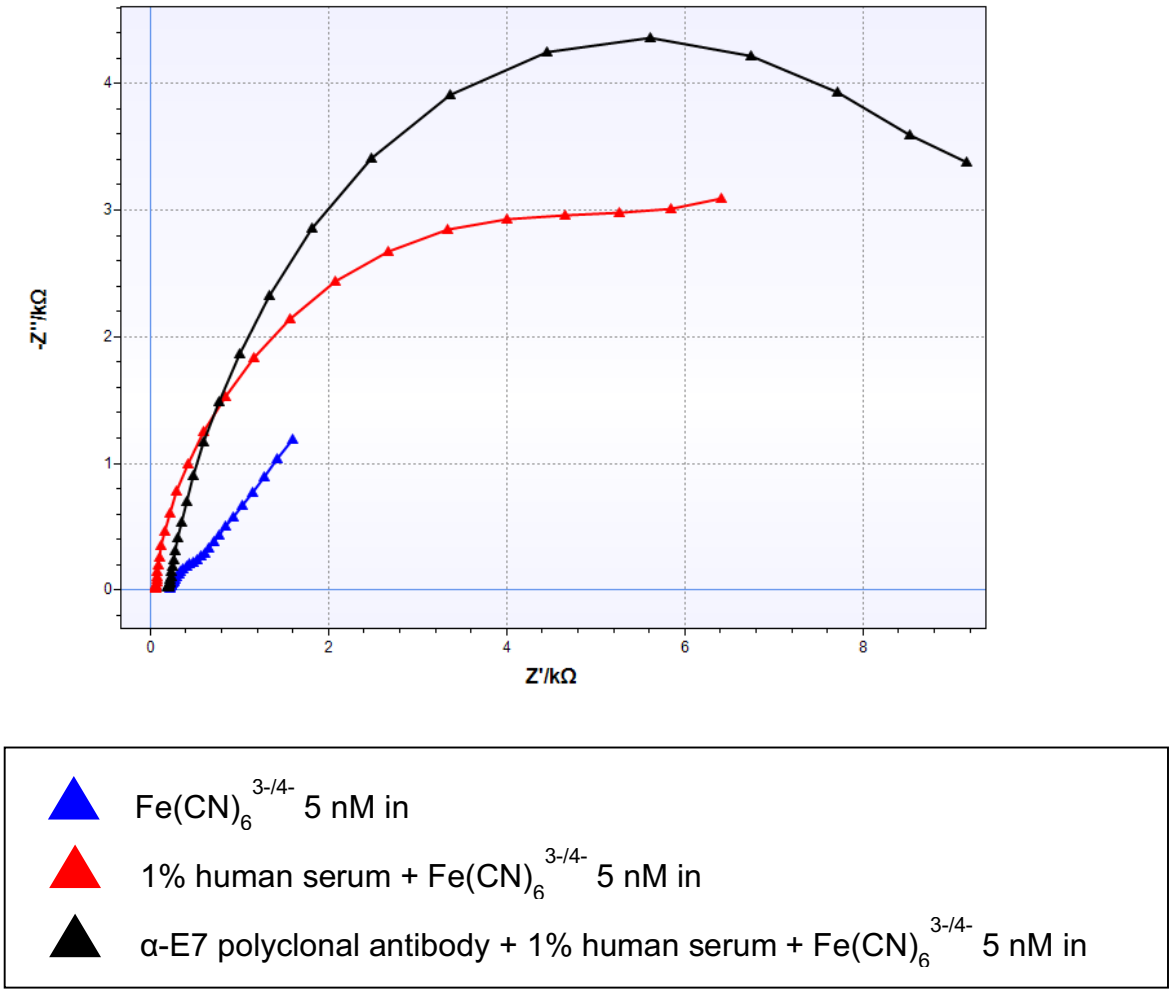

Figure 23. Impedance measurement before and after adding serum and anti-E7 polyclonal antibodies (27nM) on electrode surface functionalized with:
E7 recombinant oncoprotein+ SWCNT + 4-ATP SAM

The redox couple $Fe(CN)_6^{3-/4-}$ was used to test the electrode at the starting point (blue line), in presence of negative human serum and after adding a drop anti-E7 antibodies at different time points. The signal was decreasing in time: after an initial increase, the signal was decreasing in time instead to reach a plateau. This was probably due to the fact that the recombinant proteins were not firmly anchored to the working electrode surface.

The binding of anti-E7 antibodies to the E7 proteins was detected in parallel with a conventional techniques (ELISA) and the result was positive.

We preferred performing the experiment using polyclonal antibodies to mime human antibodies

The unstable link between recombinant proteins and the working electrode surface is probably due to non-covalent bond with CNTs, but, on the other hand, covalent bonds decrease/cover the number of epitopes.

Thus, we tested the system with different time intervals (5, 10, 15 and 20 minutes) after adding the sample to verify if the signal might improve.

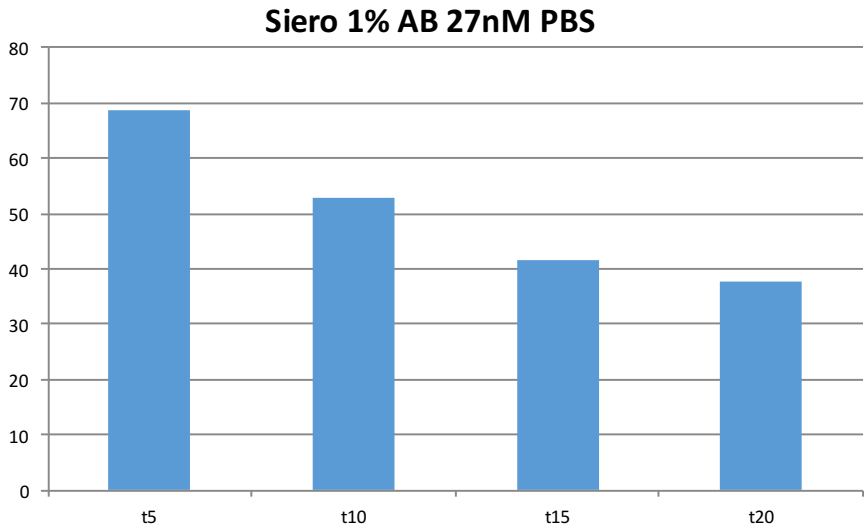

Figure 24. Impedance measurement after adding 27nM Ab in 1% serum in PBS. The measurement was repeated with different time intervals. t5= 5 min; t10= 10 min; t15= 15 min; t20= 20 min.

On the contrary, we observed that the signal decreased with time, due to a likely progressive detachment of the E7 protein from the electrode surface.

5.5 RECOMBINANT E6 PROTEIN ANALYSIS

At this point, we decided to test E6 protein and tested it with different SAMs.

The graph summarizes the results of functionalization experiments to select the best composition of SAM. We tested different percentages to obtain the most effective functionalization.

Specifically, we tested two main molecules, MUA and TOEG3 using different concentrations.

The assay was then tested in the presence of an antibody suitable to bind E6 protein.

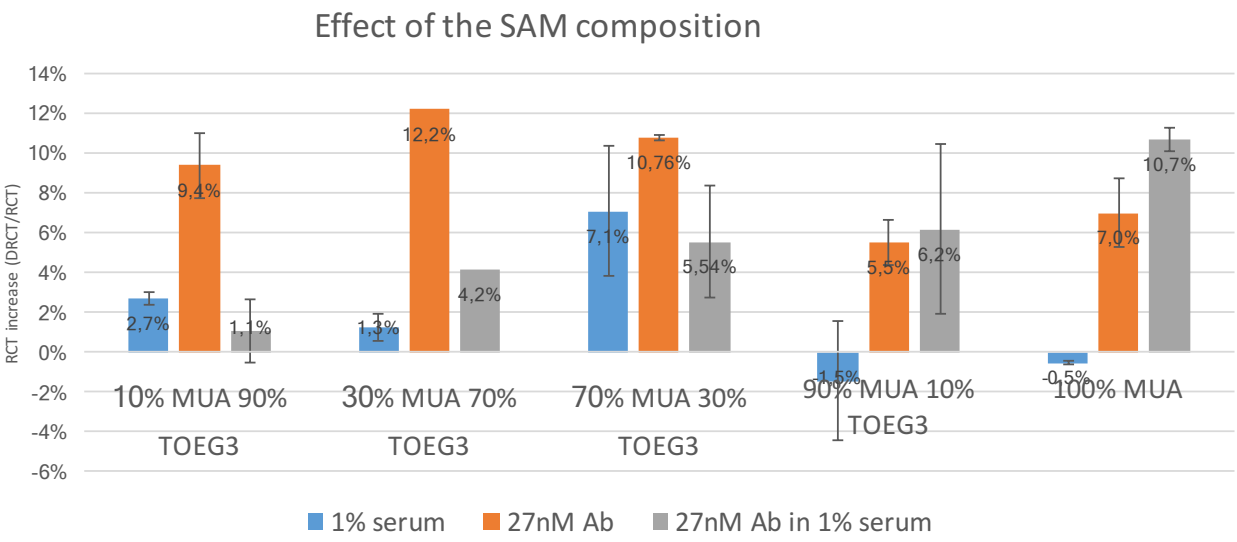

Figure 25. Impedance measurements to detect RCT increase using different SAM compositions. MUA= 11-mercaptoundecanoic acid; TOEG3= ethylene-glycol-terminated alkylthiol

We chose the second composition because the difference between negative serum in blue and antibody was the highest. Gold electrode was than modified with a mixed SAM made of 30% MUA and 70% TOEG3 (Triethylene glycol mono-11-mercaptoundecyl ether. We chose a hybrid composition to avoid steric crowding of MUA binders. Moreover, TOEG3 has antifouling properties and its role is to passivate the electrode areas not covered by MUA active molecules.

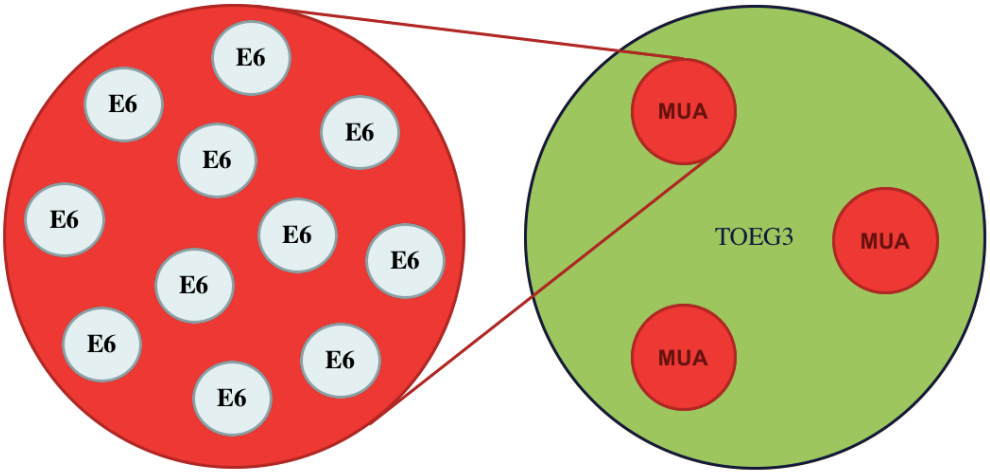

Figure 26. schematic illustration of the electrode surface functionalized with the hybrid SAM. MUA represents the active area which binds the antigen.

The carboxyl-to-amine crosslinking was performed with 1-Ethyl-3-(3-dimethylaminopropyl) carbodiimide - N-Hydroxy succinimide (EDC-NHS) to activate exposed -COOH of the MUA molecules on the electrode surface and to bind primary amine groups of HPV-E6 proteins. Then, the electrode

was coated with E6 and finally it was modified with a repellant molecule to avoid the non-specific binding of serum proteins on the electrode surface. Thereafter, a blocking procedure was performed by submerging the biosensor in glycine methyl ester solution. EIS measurements are performed by using the redox couple $Fe(CN)_6^{3-/4-}$ in PBS to measure the change of the charge-transfer resistance (R_{CT}) after each electrode modification. All the measurements were performed at open circuit potential (OCP) in the presence of 1% negative human serum or 1% negative human serum spiked with 27nM anti-E6 monoclonal antibodies; they were repeated every five minutes until the stabilization of the signal was reached.

5.6 AFM analysis

The quality of the coating was tested by AFM analysis in collaboration with NanoInnovation Lab of Elettra Sincrotrone (Prof. Casalis).

We compared the morphology of the electrode after the E6-protein binding and after a monoclonal antibody, the CD9. The SAM was 30%MUA – 70%TOEG3

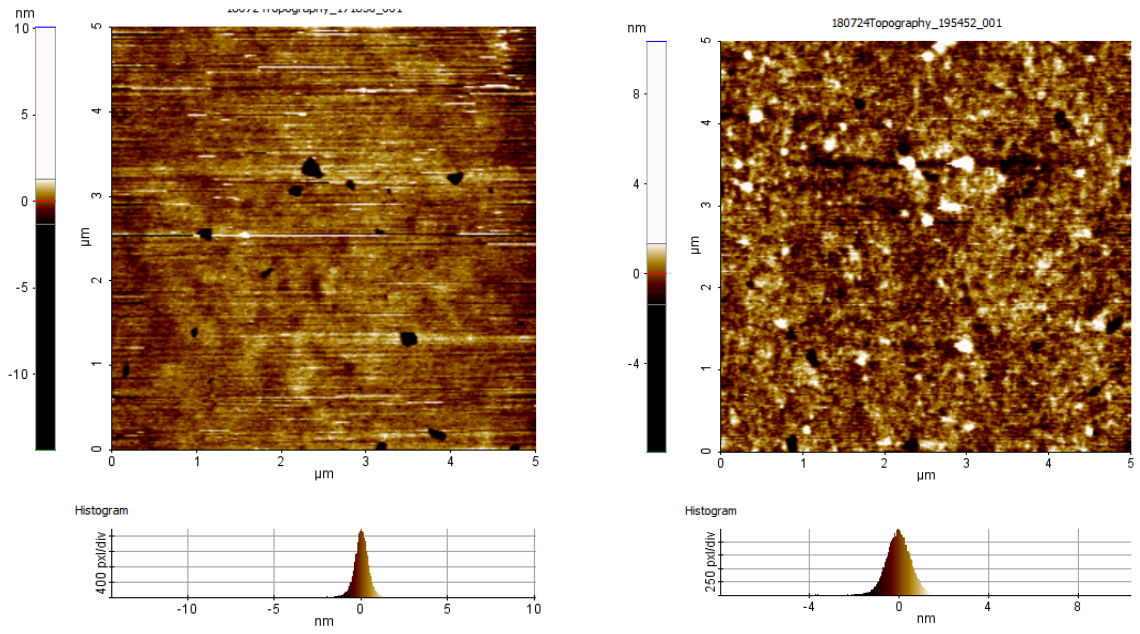

Figure 27. AFM results. On the left: surface roughness before adding CD9; On the right: Imaging surface after adding CD9 0,22mg/mL. Roughness 0.254nm and 0.528 respectively.

This experiment demonstrated that the surface roughness before CD9 adding is comparable to gold roughness, meaning that the SAM distribution is flat and quite homogeneous with no differences between MUA and TOEG3 areas in terms of thickness.

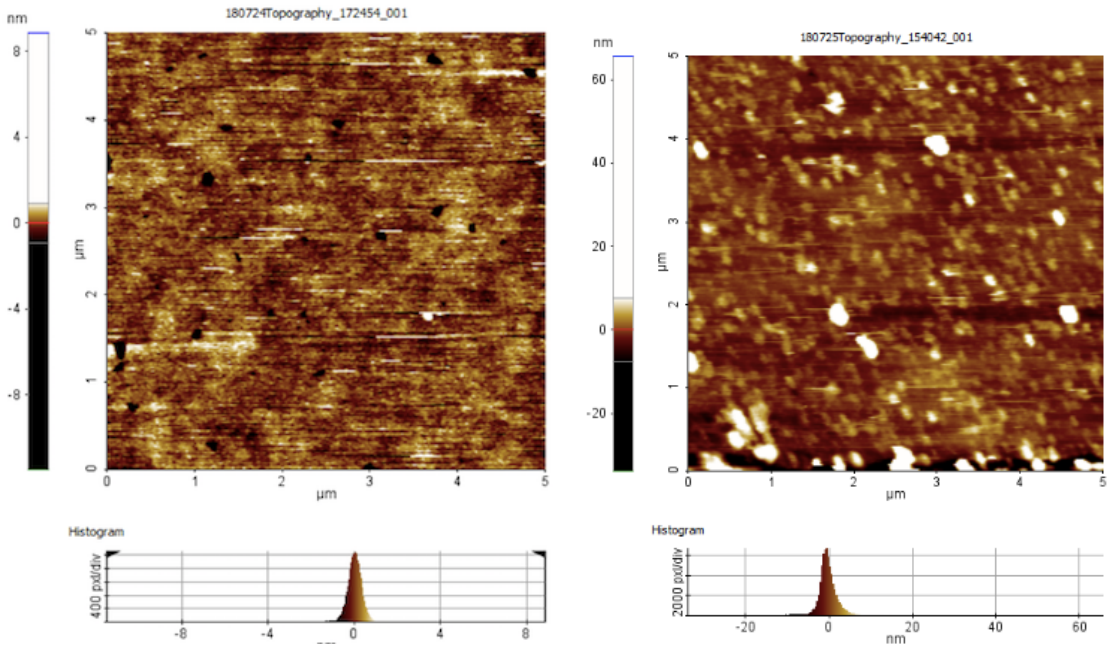

Figure 28. On the left: surface roughness before adding E6; on the right: Imaging surface after adding E6 0,35mg/mL. Roughness 0,254nm and 1.5nm respectively

The results showed that E6 oncoprotein covered the working electrode with an irregular distribution causing a clear increase in surface roughness. This is probably due to the protein-protein aggregation, which may be the cause of the small reproducibility of the EIS experiments.

5.5.1 BLOCKING SOLUTION OPTIMIZATION

At this point, we supposed that proteins aggregation on the electrode surface might be due to the lack of a blocking element. Non-specific binding to the surface can be minimized by saturating these unoccupied binding sites with a blocking reagent and it is a fundamental step to make the E6 coating homogeneous.

For this purpose, different blocking systems were tested to discriminate between positive and negative samples towards E6 antibody in ELISA. The linking between the protein and the ELISA plate is caused by hydrophobic interaction, then it is essential to saturate all the plate surface to avoid non-specific binding of serum components. A preliminary study was performed to evaluate the following eight blocking systems: 100mM Glycine methylester, 4% Goat serum, 4% Sericin, Caseine (sat) and Hek cell lysate, 670pM E7 Pepmix, 5% BSA and 3% non-fat dry milk (NFDM). All the solutions were prepared in PBS.

In the following figures (29-32) we used different sera belonging to negative patients (S54 and S60 samples), or to patients affected by HPV-driven OPSCC (SP01 and SJ01 samples).

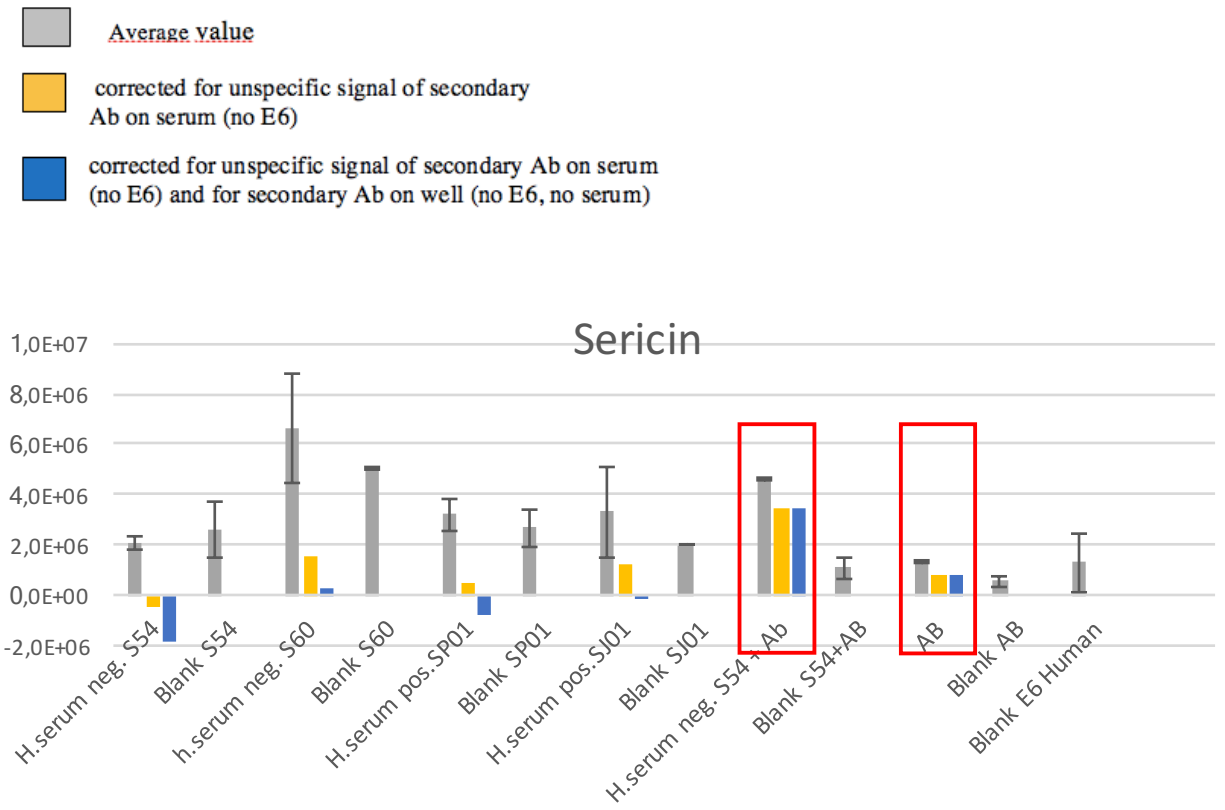

Figure 29. Sericin blocking system. The graph reports EIS measurements using different sera in order to evaluate the biosensor sensitivity in distinguishing positive and negative samples. H.=Human; neg.=negative to HPV16; pos.=positive to HPV16; AB=antibody

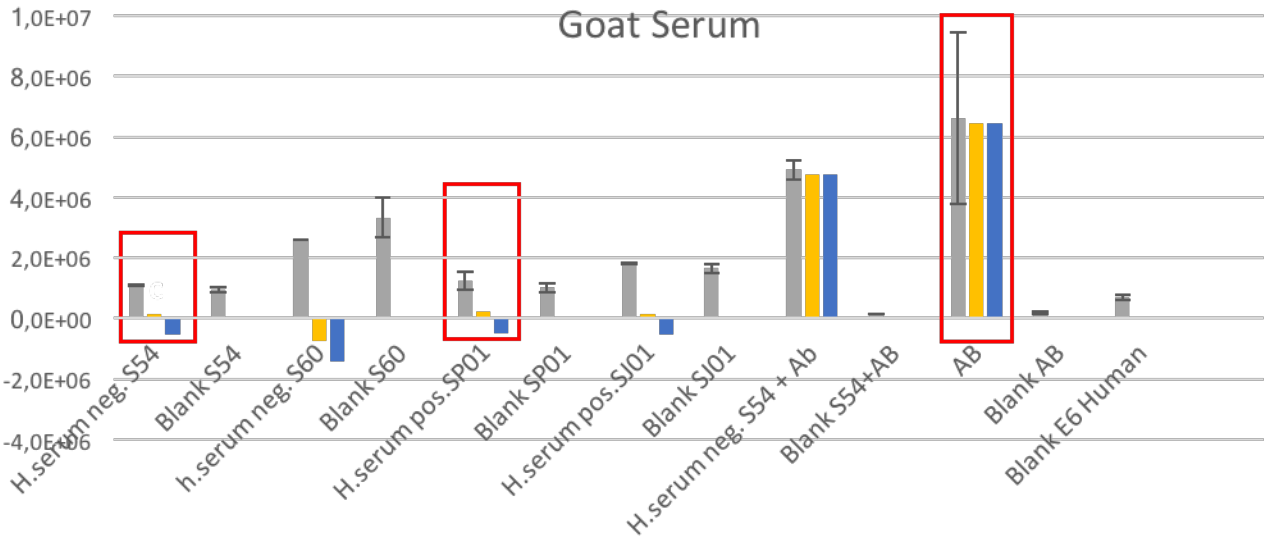

Figure 30. Goat Serum blocking system. The graph reports EIS measurements using different sera in order to evaluate the biosensor sensitivity in distinguishing positive and negative samples. H.=Human; neg.=negative to HPV16; pos.=positive to HPV16; AB=antibody.

Sericin provides very high blocking of antibodies (Figure 29), however in this blocking solution, the samples derived from the patients appeared lower than the synthetic sample containing serum and antibodies: this may be the result of a non-specific binding between antibodies non anti-E6 on the well. On the contrary, goat serum (Figure 30) gives a good result for the synthetic antibodies but there are no differences between samples derived from patients affected by HPV-driven OPSCC or healthy volunteers.

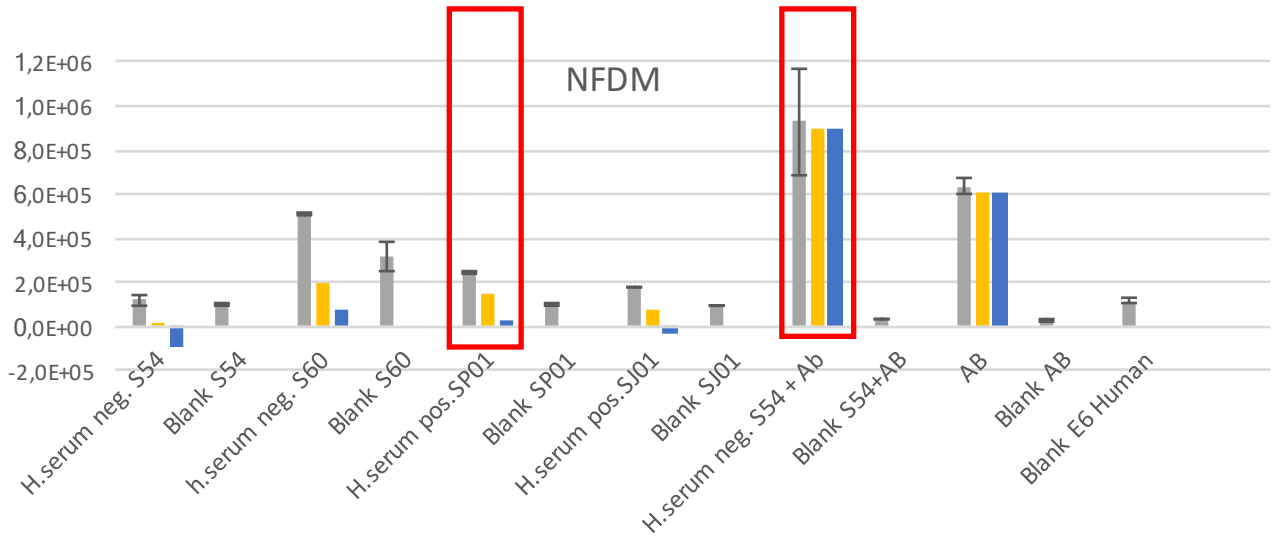

Figure 31. Non-fat dry milk (NFDM) blocking system. The graph reports EIS measurements using different sera in order to evaluate the biosensor sensitivity in distinguishing positive and negative samples. H.=Human; neg.=negative to HPV16; pos.=positive to HPV16; AB=antibody

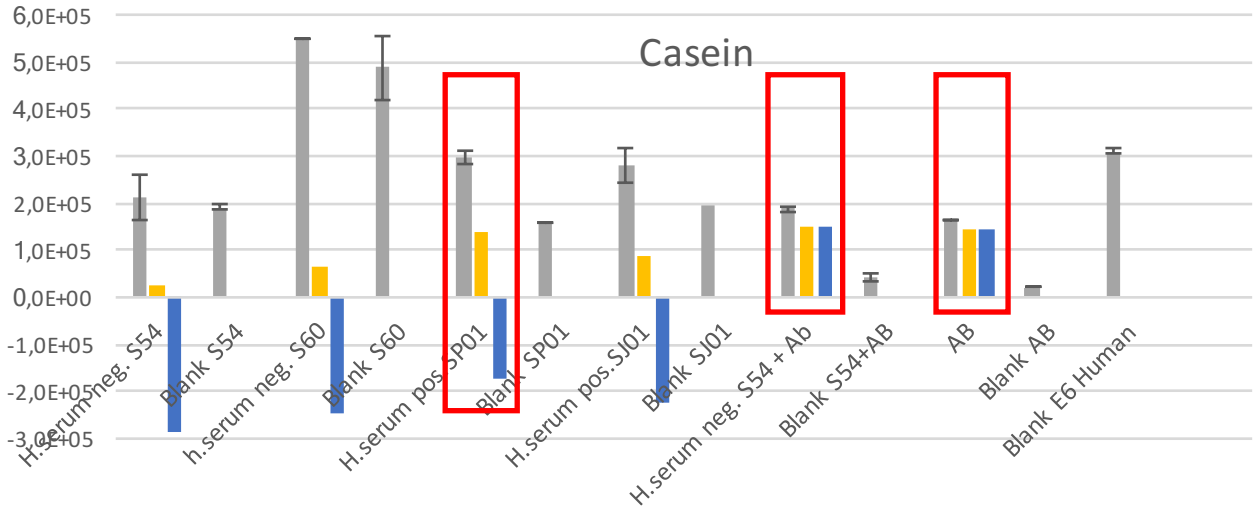

Figure 32. Casein blocking system. The graph reports EIS measurements using different sera in order to evaluate the biosensor sensitivity in distinguishing positive and negative samples. H.=Human; neg.=negative to HPV16; pos.=positive to HPV16; AB=antibody

According to the experimental data obtained, the best blocking systems were 3% NFDM and saturated Casein in a PBS solution for 2h at 37°C .

These systems allow to discriminate properly between patients affected and healthy volunteers in ELISA. Thus, we selected the Casein blocking system to carry on the experiments of the project and we tested this system in EIS.

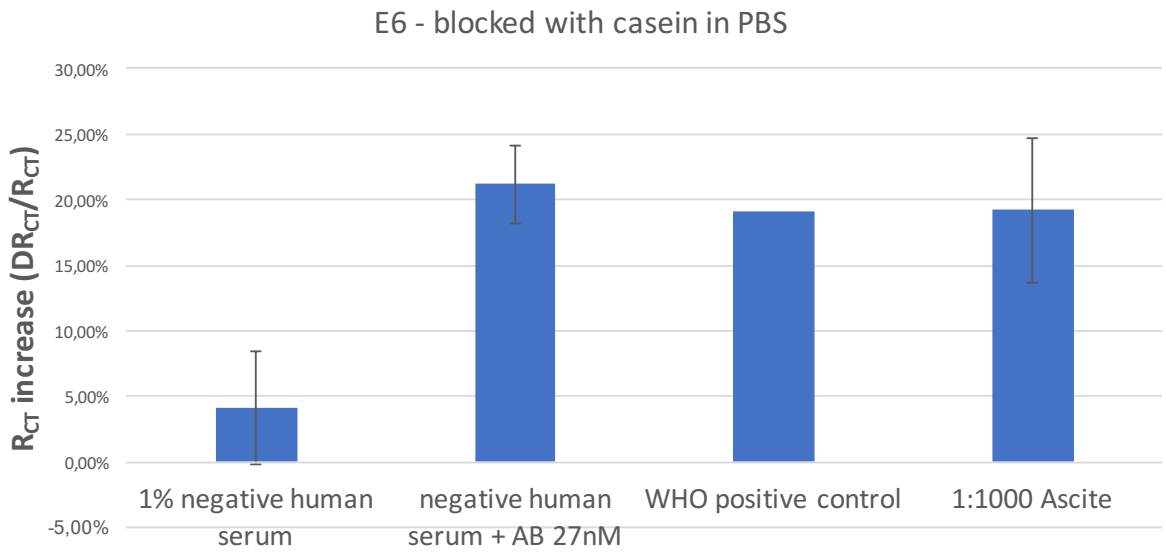

Figure 33. Casein blocking system: the graph reports the Rct increase for different samples in order to verify the discriminating ability of the system. We observed a statistically significant 4-fold difference between negative and spiked samples.

The comparison between negative and spiked samples showed an R_{CT} increase for the latter; the difference was high but not enough to completely discriminate the samples, probably caused by the strong interaction between the serum proteins and the electrode surface.

5.5.2 REDUCING AGENTS TO COUNTERACT AGGREGATION

At this point, we reasoned about another solution to avoid the protein-protein aggregation. We hypothesized that a treatment with a strong reducing agent as Tris (2-carboxyethyl) phosphine (TCEP), before the E6-protein coating, could have been helpful to reduce the disulphide bridges among proteins, allowing a homogeneous coverage of the electrode surface.
Other experiments were conducted also using TCEP as reducing system. We found that this method could indeed improve the sensitivity of the system.

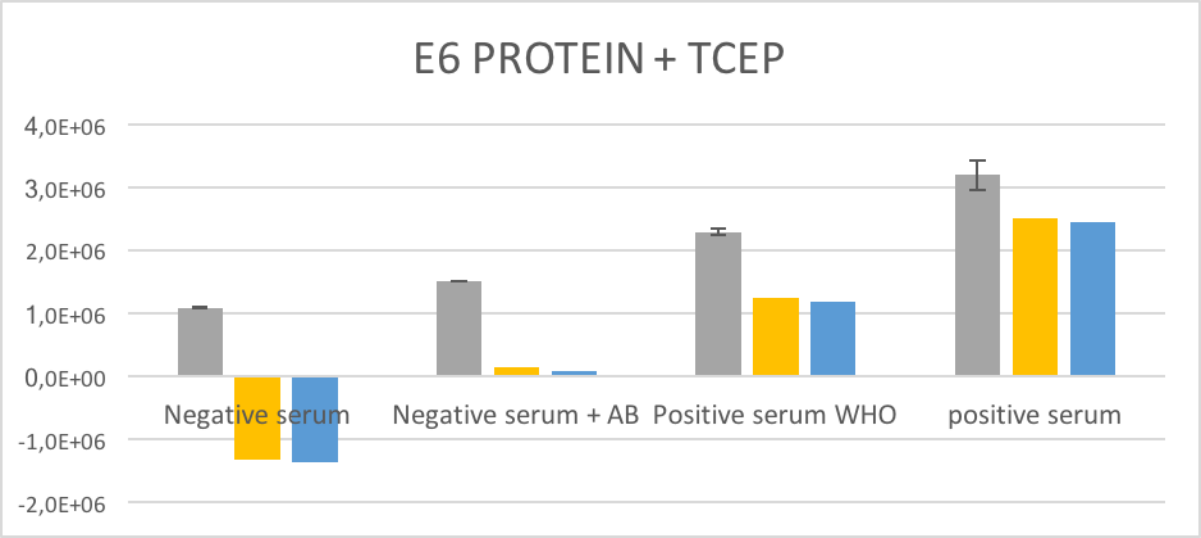

Figure 34. Tris (2-carboxyethyl) phosphine (TCEP) reducing agent to counteract protein-protein aggregation. The positive serum on the right showed the greater R_{CT} increase compared with negative sera.

5.6 HPV16-E6 Protein stability analysis

Protein E6 stability was one of the key factors that could be involved in protein aggregation on the electrode. We tested different E6-proteins because there are many difficulties in E6 oncoprotein production: it is scarcely stable, and it showed a the tendency to change rapidly; moreover it can spontaneously assemble into large organized ribbon structures and it has an instable structure. Different batches of protein have been produced applying different protocols that are available in literature and thanks to a collaboration with dr. Paola Storici, Head of the Protein Production Facility, Elettra Elettra - Sincrotrone Trieste.

NAME	DATE	PROTOCOL	[E6] / (mg/ml)
E6VF01_ AL1	14/01/2019	1	1.19
E6VF01_AL2+3	14/01/2019	1	1.25
E6VF02	28/01/2019	2	0.41
E6VF03	01/02/2019	3	0.19
E6VF04	01/02/2019	4	0.48
E6VF05	06/02/2019	4	0.44
E6VF06	06/02/2019	3	0.44
E6VT01	03/01/2019	5	0.02

E6VT02	14/01/2019	6	0.33
E6VT03	17/01/2019	7	0.37
E6VT04	17/01/2019	8	0.93

Table 4. The table summarizes the correspondence between protocol number and E6 protein type.

The Table 4 summarizes all the proteins we tested and below we reported the protocols used.
Protocol 1 starts with dialysis in PBS, followed by TCA precipitation and wash with 70% cold EtOH; after that the protein was resuspended in PBS + 1% SDS.
Protocol 2 differs from the first because it lacks dialysis and PBS contains 0.1% SDS.
The third protocol differs from the previous one because it starts with dialysis in PBS adding 2mM DTT.
The 4th protocol foresees only dialysis in PBS adding 2mM DTT and 0.1% SDS.
In the protocol 5, after TCA precipitation, the washing steps is performed in 100% cold Acetone. Moreover, E6 is resuspended in 10mM MES pH 6.5.
The 6th protocol maintains wash in Acetone, as protocol 5, but the purified protein is resuspended in the previous buffer (PBS + 1% SDS), used in protocols 1, 2, 3, and 4..
In protocol nr.7 20 mM DTT has been added to Acetone and cell pellet resuspension occurs again in a different buffer: 100mM HEPES pH 7.4 + 1% SDS.
Protocol nr.8 preserves the use of 20 mM DTT but it foresees the use of previous buffer to resuspend the protein (PBS + 1% SDS)

All the proteins were tested with a standard protocol in ELISA and as a target we applied a serial dilutions of antibodies diluted at different known concentrations.

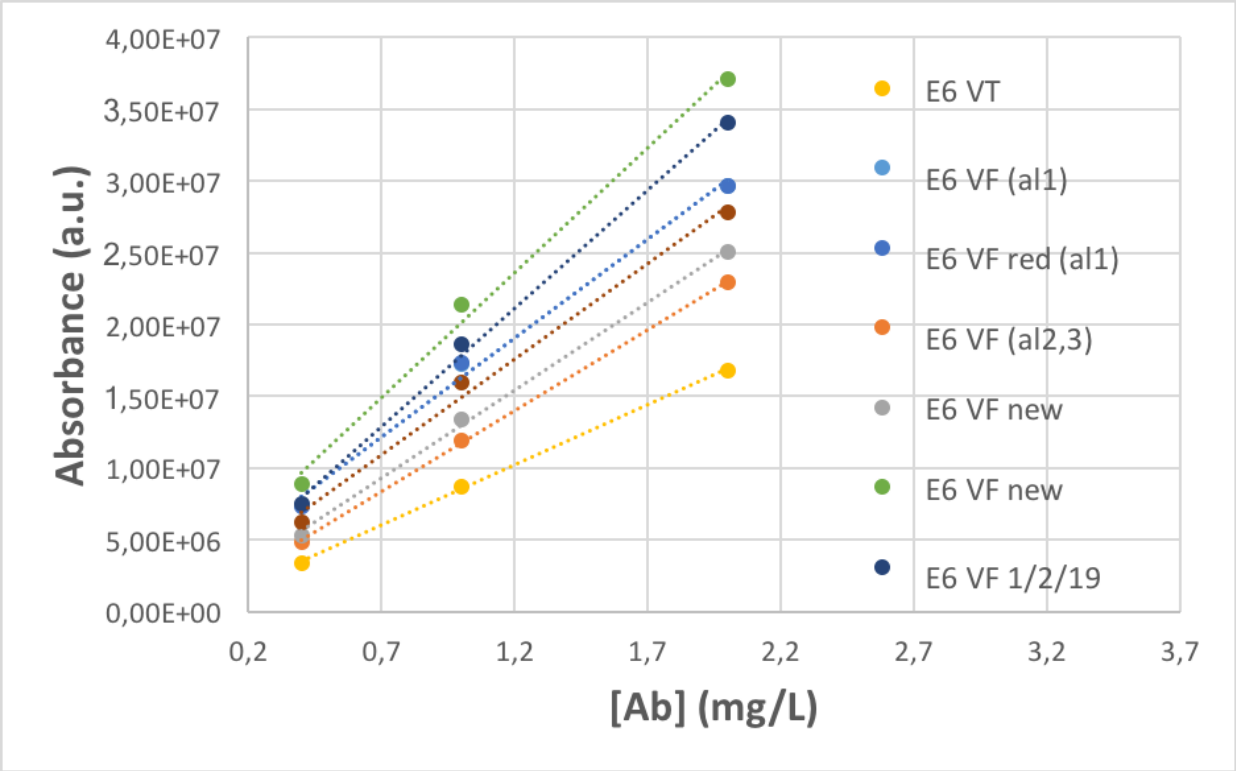

Figure 35. Experimental conditions: Pawlita's protocol – 0.2% casein in PBS-T (blocking solution) filtered before use, OptiPlate-96, White 96-well Microplate (PerkinElmer), kit Femto Elisa, IgG-HRP secondary Ab. E6 VF red refers to E6 reduced by a 100x excess of TCEP (20', rt).

As shown in figure 35, although all proteins are able to give a signal proportionate to the amount of antibody, already it is evident a strong variability in terms of signal intensity in ELISA.

Afterwards, we tested the same proteins in EIS (figure 36) using different electrodes with a positive and a negative control in different conditions.

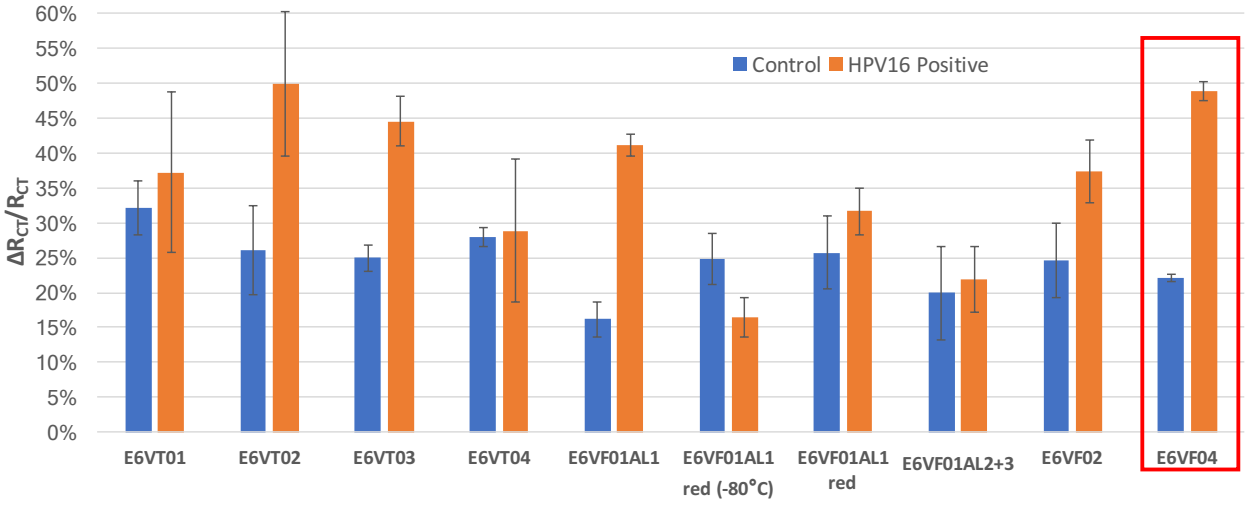

Figure 36. Measurements performed in 5mM $[Fe(CN)_6]^{3-/4-}$ in PBS, OCP. Error bars refer to standard errors calculated on 2-3 independent measurements. E6VF red refers to E6 reduced by a 100x excess of TCEP (20', rt). E6VF red (-80) refers to E6 VF stored at -80°C with an excess of TCEP.

We obtained the best results in terms of ability to distinguish the positive control by means of the protein E6VF04, produced with the protocol n.4. At this point, E6VF04 was repeatedly tested to assess the system reproducibility. In figure 37 we reported the results obtained comparing the positive sample (P01) and the negative one (s54) in different days.

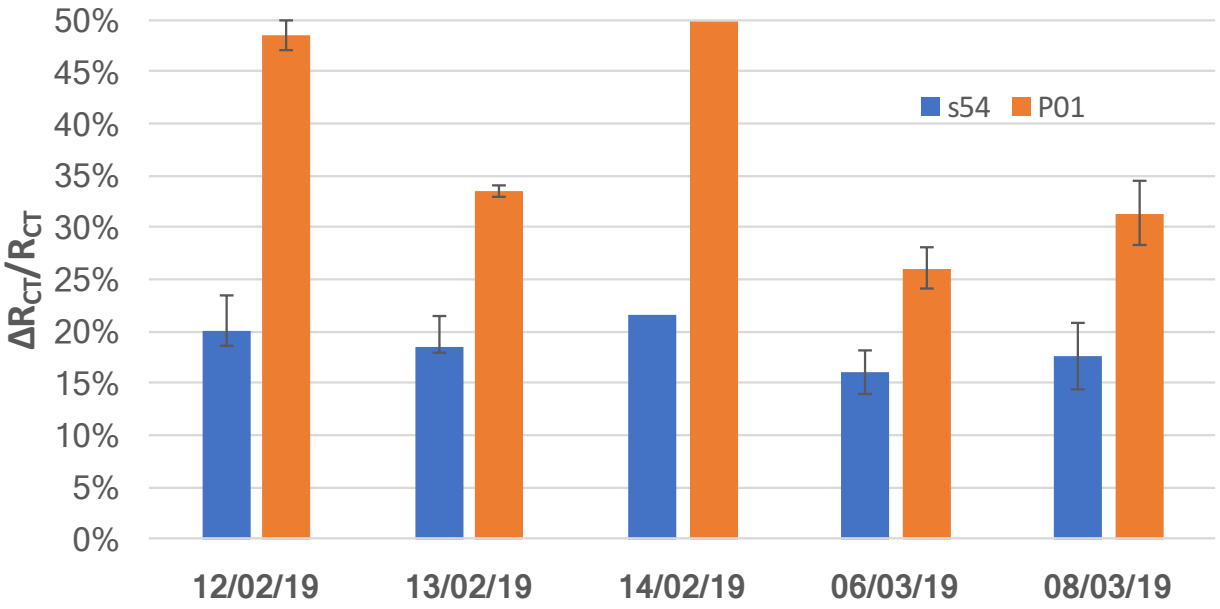

Figure 37. Measurements performed in 5mM [Fe(CN)6]3-/4- in PBS, OCP. E6VF04 has been used for these experiments. Error bars refer to standard deviations calculated on 2 independent electrodes.

Although the difference in signal intensity between the analysed samples was always statistically significant, the variability among experiments was quite high.

In fact, signal increase correlated to 1% negative serum remains almost stable over the time, while that one correlated to 1% HPV16 positive serum decreases.

We supposed that the signal stability might benefit from coating an increased amount of protein on the electrode surface.

Previous experiments were usually performed with 20ng/uL E6VF04. Therefore, we tested different E6VF04 concentrations with and without blocking: we observed that the background was similar when the blocking system was applied (Figure 38).

However, the increase of protein concentration does not correspond to a respective increase in signal, meaning that the electrode is saturated yet.

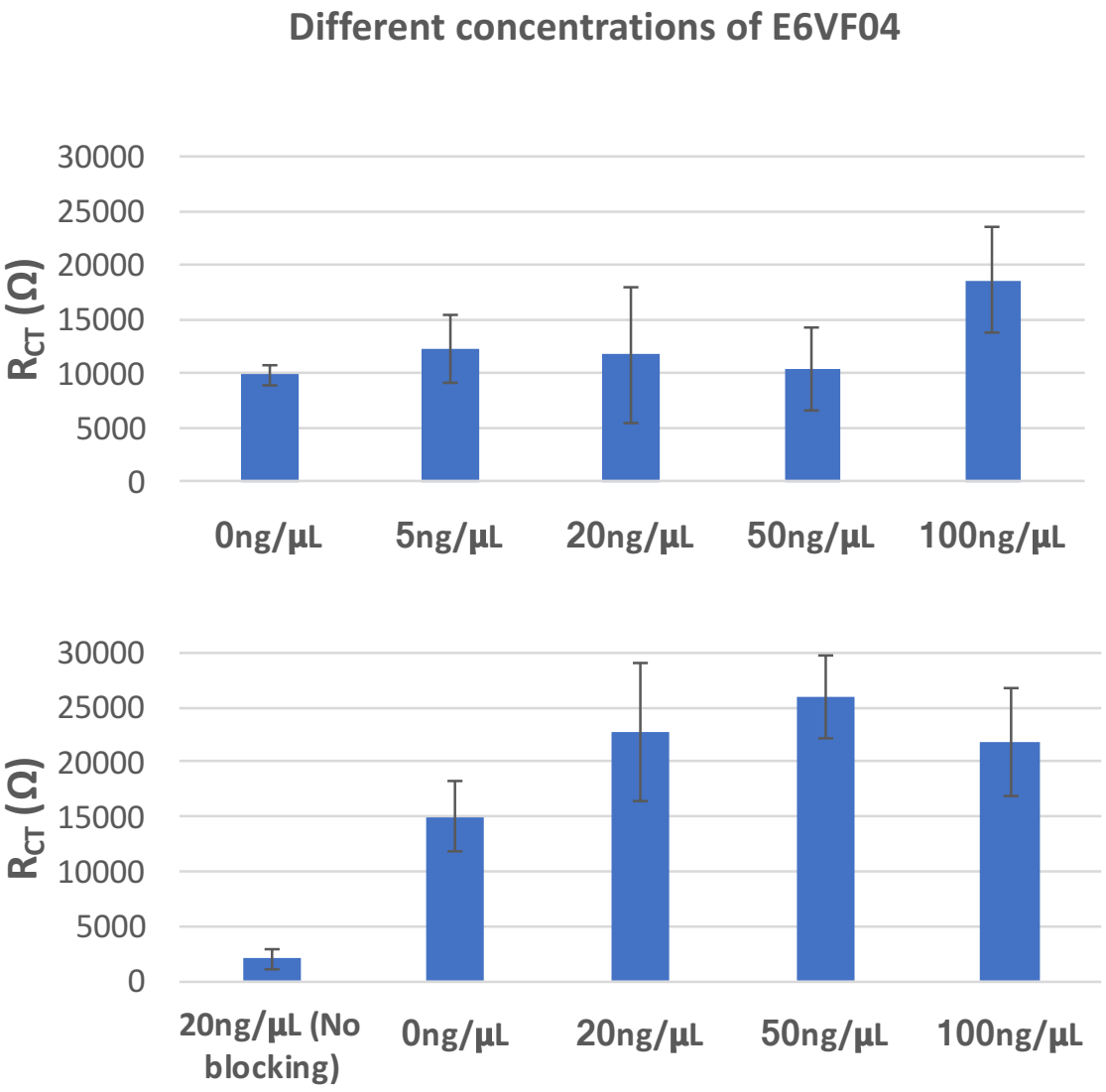

Figure 38. Measurements performed in 5mM $[Fe(CN)_6]^{3-/4-}$ in PBS, OCP. E6VF04 has been used for these experiments. Error bars refer to standard deviations calculated on 2 independent electrodes.

To exclude that the instability of the protein was due to a sort of freeze and thaw effect, we tested the response over time of the same protein batch after repeated freeze-thaw cycles. We noted that the reproducibility is low, although in each experiment the positive sample was correctly identified.

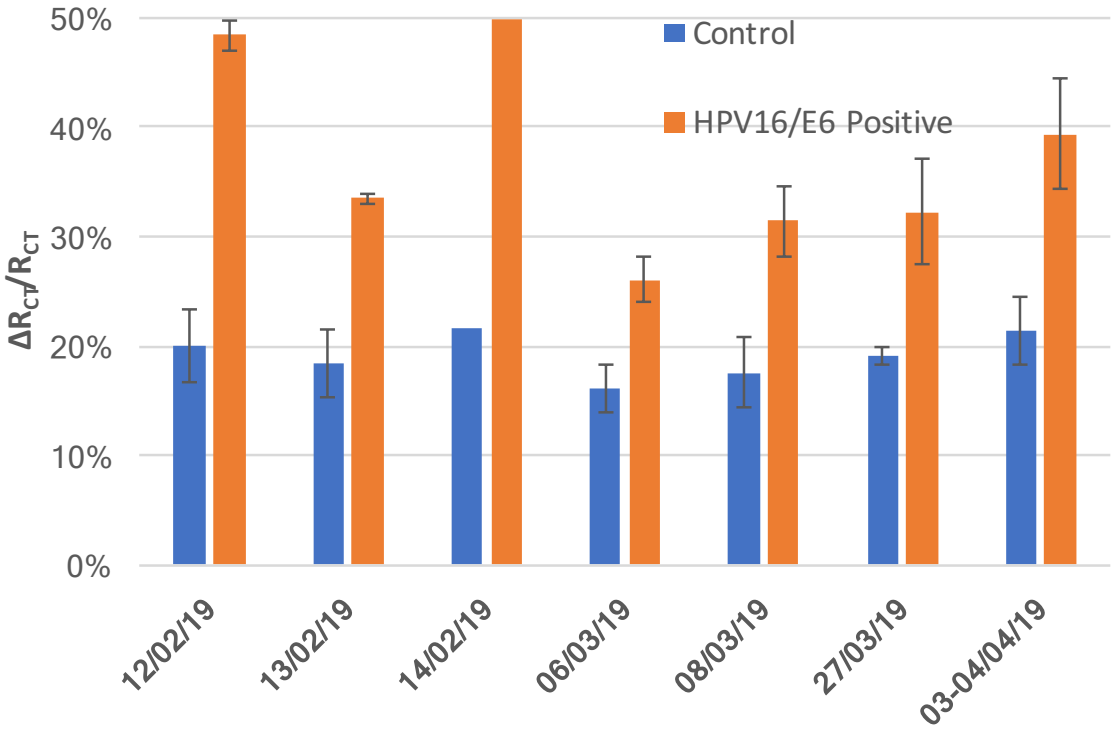

Figure 39. Measurements performed in 5mM $[Fe(CN)_6]^{3-/4-}$ in PBS, OCP. Error bars refer to standard errors calculated on at least 2 independent measurements. E6VF04 has been used for these experiments. Control=s54, HPV16/E6 Positive=sP01 R_{CT} recorded after 10 minutes since the addition of 1% sample.

5.7 Clinical pilot study

Finally, we decided to assay the definitive protocol testing a wider pool of human sera.

We collected a pool of OPSCC samples made of 14 HPV16-negative sera and 14 HP16-positive human sera.

Initially, we conducted a standard ELISA to detect the presence of anti-E6 antibodies in these sera.

The results are reported in figure 40: we noted that positive samples presented higher anti-E6 IgG titers.

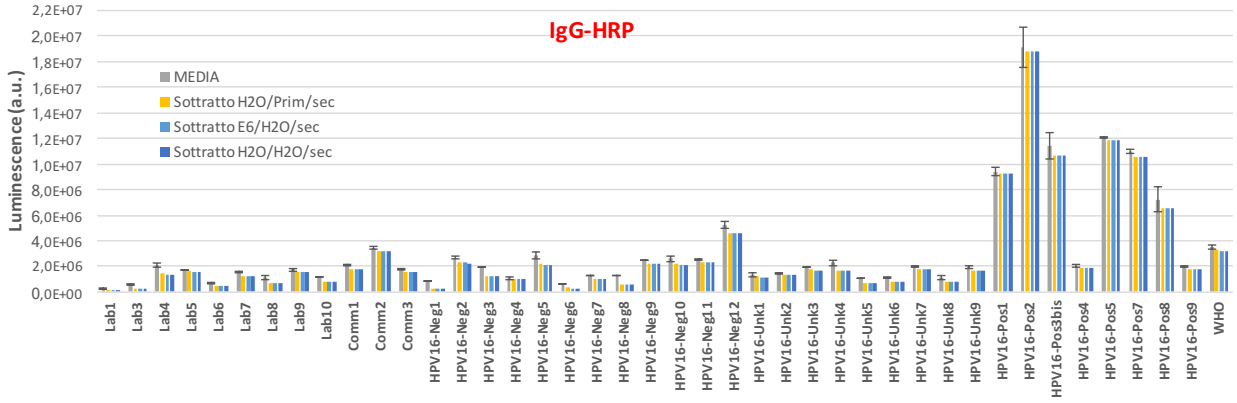

Figure 40. Experimental conditions: Pawlita's protocol – 0.2% casein in PBS-T (blocking solution) filtered before use, OptiPlate-96, White 96-well Microplate (PerkinElmer), kit Femto Elisa, IgG-HRP secondary Ab.
E6VF04 in 4M urea (before the dilution in CB) has been used. Error bars refer to standard errors calculated on 2 independent measurements. Lab1-10 and Comm1-3 are sera from volunteers to constitute the negative pool as control. HPV16-Neg1-12 and HPV16-Unk1,5,6,8 are OPSCC patients' sera negative for HPV; HP16-Pos1-9and HPV16Unk2,3,4,7,9 are HPV-positive sera.

At this point, therefore, we chose randomly 3 HPV-positive and 3 HPV-negative samples that were initially tested (Figure 41) and we noted a statistically significant difference in terms of Rct between positive and negative cases (pvalue < 0.05. T-test).

The experiments reported in Figure 41 were conducted using the WHO standard as positive control. Polyclonal anti-HisTag antibody has been used to verify the coating of HPV16-E6 on the electrode surface. The HPV infections have been confirmed by pyro-sequencing of the extracted DNA.

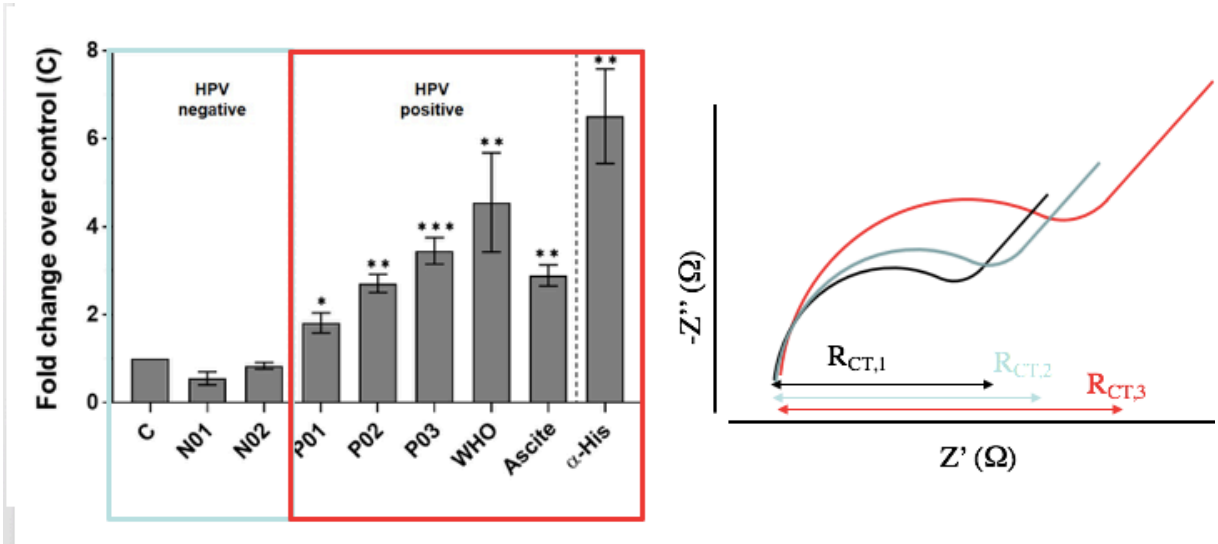

Figure 41: Fold $\Delta R_{CT}/R_{CT}$ change (over the $\Delta R_{CT}/R_{CT}$ of the control negative sample, C) after the addition of 1% (C, N01, N02, P01, P02, P03) sera or 1% WHO standard serum (pool of different HPV positive sera) or 0.1% (Ascite) serum or 0.1% polyclonal anti-HisTag antibody (α-His) in 5 mM $[Fe(CN)_6]^{3-/4-}$ in PBS solution. EIS measurements have been

performed applying a sinusoidal AC voltage of 10 mV (peak-to-peak voltage) in amplitude at the frequency range 0.1 ÷ 1000 Hz at the OCP. Statistical significance was assessed by T-test over serum C. Error bars refer to the standard errors calculated on indipendently prepared electrodes. N01 and N02= negative samples nr.01 and 02; P01,P02 and P03= positive samples nr.01,02 and 03. On the right, $R_{CT,2}$ and $R_{CT,3}$ correspond to negative and positive samples R_{CT} measurements, respectively.

Figure 41 shows a significant increase of $R_{CT,3}$ compared to the resistance detected with negative samples.

Since this pilot experiment is comforting, we are going to apply Pawlita's protocol condition as the experiment shown in Figure 40 to the whole pool of sera.

6. DISCUSSION:

The aim of the project was to optimize a biosensor for the detection of HPV antibodies against HPV E6 and E7 oncoproteins using the Electrochemical Impedance Spectroscopy (EIS) technique.

Scientific literature has underlined through several studies that HPV antibodies present in serum can represent a good diagnostic and prognostic biomarker for OPSCC; however, they are still not exploited in clinical practice. This can be partially explained by the fact that there are no Point-Of-Care systems for HPV antibodies efficient detection in serum, that could be executed by the clinician itself at ambulatory level. EIS could represent a convenient tool for the development of such application.

The impedance depends on the layer present on the electrode; therefore, the idea was to functionalize electrodes with a first layer of recombinant HPV oncoproteins to be used as a “bait” to capture antibodies when a drop of patient’s serum/blood is deposited on the electrode surface.

The direct monitoring of the conjugated layer formation between antigen and antibody provides a favourable detecting system, with a high signal-to-noise ratio, an easy signal detection and a rapid data analysis. However, regenerate the biological surface does not allow to perform measurements in succession because the procedure becomes time consuming and not reproducible. Moreover, the regeneration process might damage the surface causing the bioreceptor detachment. This represents the main limitation in immune-biosensor production when the complex antibody-antigen to be detected has high affinity constants.

The structure should be accurately planned to minimize the unspecific bond between other blood components on the electrode surface.

Firstly, E7 Pepmix was used as a bioreceptor for the electrode preparation. In literature, the use of Pepmix in HPV-associated cancers is not new, but it was mostly used to expand HPV16 E6/E7-directed T-cell lines from patients with HPV16- cancers. The purpose of the authors was to identify

mechanisms by which ex vivo stimulation of T cells could reactivate and expand tumor-directed T-cell lines from HPV cancer patients for subsequent adoptive immunotherapy [72]. Differently, in our study, the surface of gold working electrodes was functionalized with 4-ATP, single wall carbon nanotubes and finally it was coated with E7 pepmix.

The redox couple $Fe(CN)_6^{3-/4-}$ was used to test the electrode and the signal, detected as R_{CT} change, was measured before and after adding a solution containing anti-E7 antibodies in presence of 1% serum. The experiments in EIS conducted with Pepmix did not detect the interaction antibody-antigen, while in ELISA the signal was present. This result means that the system is not valid to detect antibodies because there was a strong unspecific interaction between Pepmix and serum proteins.

Moreover, Pepmix has the advantage to be cheap and stable, however the structure corresponds only to linear epitopes so antibodies that recognize conformational epitopes are lost.

So, we switched to test recombinant proteins as bioreceptor, starting with E7 oncoproteins, and using polyclonal antibodies to mime human antibodies.

It was possible to observe an increase of the impedance signal in presence of antibodies in serum. However, after an initial increase, the detected signal was decreasing in time instead to reach a plateau and that was probably because the recombinant proteins were not firmly anchored to the working electrode surface and the interaction between the electrode surface and the other blood elements might displace the bond with antibodies. The binding of anti-E7 antibodies to the E7 proteins was detected in parallel with a conventional techniques (ELISA) and the result was positive. The unstable link between recombinant proteins and the working electrode surface is probably due to non-covalent bond, but, on the other hand, covalent bonds might decrease/cover the number of epitopes.

Recombinant proteins allow to recognize antibodies that bond conformational epitopes; nevertheless, the production is not easy, particularly in HPV E6 due to accentuate instability of the structure [73].

We decided to produce HPV16 E6 with different protocols, and afterwards, we tested E6 oncoproteins with mixed SAMs made of 30% MUA and 70% TOEG3 to coat the working electrode surface that was modified with blocking systems to prevent the non-specific binding of serum proteins. We chose to make a hybrid SAM to avoid steric hindrance of MUA binders. Moreover, TOEG3 has antifouling properties and its role was to passivate the electrode areas not covered by MUA active molecules [56,74]. The activation of exposed -COOH of the MUA molecules on the electrode surface was performed with EDC-NHS to make this group reactive to bind primary amine groups of HPV-E6 proteins. The comparison between negative and spiked samples showed an R_{CT} increase for the latter. The difference was high enough to discriminate the samples, but we registered a strong interaction between the serum proteins and the electrode surface.

At this point, we decided to perform AFM analysis, conducted in collaboration with the group of prof. Loredana Casalis (NanoInnovation Lab of Elettra Sincrotrone, Trieste) to compare the morphology of the electrode after binding E6 protein or another monoclonal antibody (CD9). The results showed that the binding with E6 oncoprotein determined an increase of the roughness with an irregular distribution on the electrode surface highlighting protein aggregation, which may be the cause of the limited reproducibility of the EIS experiments.

Then, we focused on understanding which was the cause for protein aggregation and hypothesize that a better blocking system could be helpful to achieve a homogenous coating of the protein on the electrode surface. We therefore proceeded testing different blocking systems to better discriminate between positive and negative samples. The linking between the protein and the ELISA plate is caused by hydrophobic interaction, then it is essential to saturate all the plate surface to

avoid non-specific binding of serum components. According to the experimental data obtained, the best blocking systems were 3% NFDM and satured Casein in a PBS solution for 2h at 37°C.

Glycine methylester in EIS could be replaced by the most effective blocking systems in ELISA (casein) to drop down non-specific signal from serum proteins, thus amplifying the difference between positive and negative samples. To optimize the blocking system, thanks to the experience had in Heidelberg as visiting scientist in the group of Professor Michael Pawlita at the German Cancer Research Center (DKFZ), we adjusted the protocol for blocking procedure to improve the system avoiding the "over-blocking" of the electrode.

Finally, with the best version of the prototype, we conducted an initial clinical pilot study on human sera, where we investigated the seropositivity for HPV16 E6 as a marker of HPV16 positive OPSCC [75,76].

Nowadays the HPV status in clinical samples is usually tested with polymerase chain reaction (PCR) assay for viral DNA, Southern blot, in situ hybridization, and immune-histochemical staining performed on biopsies. However, antibody response to the viral proteins E6 and E7 was strongly associated with the development of cancer [77] while seropositivity is rare (<1% prevalence) in cancer-negative subjects [78].

Thus, numerous authors have explored several risk-stratification tools, such as E6-seropositivity, that is under active examination and could enable studies to solve the current challenges of diagnose early stage HPV-driven OPSCC and feasible screening modalities [79]. E6-seropositivity precedes cancer diagnosis by 5–15 years, emphasising its potential utility as a screening biomarker [80] and it seems also strongly associated with improved progression-free survival in patient cohort with HPV16+ tumours [81].

Assays to quantify HPV-specific antibodies were based on Enzyme Linked Immuno-Sorbent Assays (ELISA) which requires specialized laboratory and personnel, it is quite expensive, complex and time-

consuming. Moreover, it requires pre-steps of sample processing, that can cause proteins denaturation and bioactivity modification.

Although the limited sample size, this study presented promising results. Preliminary data on the technology showed that it is possible to detect HPV16 anti-E6 antibodies by means of an EIS-based biosensor with a low detection limit (LOD) of 5-10 ng/ml of antibodies (60 picomolar), which is an encouraging result for an impedence-based biosensor.

The clinical study has been conducted in accordance with Helsinki declaration on human sera collected from 12 volunteers to constitute the negative pool as control and from 28 patients affected by OPSCC as test group. In each measurement, the WHO serum was adopted as positive reference. The test group was enrolled at the Otorhinolaryngology clinic, Cattinara hospital, in Trieste and it was composed of patients surgically treated for OPSCC from 2016 to 2019. Patients were informed about the purpose of the study and they gave their consent to collect and analyse blood. The results showed that the biosensors had the potential to discriminate between HPV-positive and -negative sera using just a drop of serum and this sensitivity makes the technique potentially indicated in a POC system. Nevertheless, the huge instability of the recombinant E6 oncoprotein was the limiting factor that influenced the reproducibility of this system. Therefore, further studies are required to modify the electrode surface thus improving the blocking conditions and to evaluate another electrode surface, e.g. a flat gold surface, as the nanoelectrode arrays (NEAs). Among different detection systems, EIS-based biosensor showed highly effectiveness, thanks to the great sensitivity and selectivity of the analysis, giving the opportunity for miniaturisation in portable devices and the possibility to perform an automated non-stop single or multi-analytes monitoring. The structure made of a mixture of nanostructures and bioprobes provides further advantages in terms of sensitivity, specificity and measurement reproducibility. Furthermore, EIS allows the monitoring of the addition of each layer on the sensing surface,

including nano- and bio- materials, such as SAM layers, carbon nanotubes and finally the bioreceptors.

DNA-based EIS biosensors with limit of detection in aM range are reported in literature for the detection of small molecules [82] as well as for HPV16 biomarkers [83,84]. However, a reliable HPV16 biosensor detecting anti-E6 and anti-E7 is not reported and, despite the body of research currently available, no POC biosensors are commercially available and can compete with more complex techniques in terms of sensitivity and limits of detection, to the best of our knowledge. Antibodies are quite big molecules (about 150.000 Dalton) therefore their presence on the electrode surface is detectable by measuring the variance of electrical capacity. This low-cost technology may allow to build a very easy test, that avoids washing and handling steps, implying a strong reduction of time and cost.

7. References

1. Global Burden of Disease Cancer C, Fitzmaurice C, Allen C, Barber RM, Barregard L, Bhutta ZA, et al. Global, regional, and national cancer incidence, mortality, years of life lost, years lived with disability, and disability-adjusted life-years for 32 cancer groups, 1990 to 2015: a systematic analysis for the global burden of disease study. JAMA Oncol 2017;3:524e48.
2. Chaturvedi AK, Engels EA, Pfeiffer RM, Hernandez BY, Xiao W, Kim E, et al. Human papillomavirus and rising oropharyngeal cancer incidence in the United States. J Clin Oncol 2011;29:4294e301.
3. Plummer M, de Martel C, Vignat J, Ferlay J, Bray F, Franceschi S. Global burden of cancers attributable to infections in 2012: a synthetic analysis. Lancet Glob Health 2016;4:e609e16.
4. Giuliano AR, Lu B, Nielson CM, Flores R, Papenfuss MR, Lee JH, et al. Age-specific prevalence, incidence, and duration of human papillomavirus infections in a cohort of 290 US men. J Infect Dis 2008;198:827e35.
5. Fakhry C, Westra WH, Li S, Cmelak A, Ridge JA, Pinto H, et al. Improved survival of patients with human papillomavirus-positive head and neck squamous cell carcinoma in a prospective clinical trial. J Natl Cancer Inst 2008;100:261e9.
6. Gillison ML, D'Souza G, Westra W, Sugar E, Xiao W, Begum S, et al. Distinct risk factor profiles for human papillomavirus type 16-positive and human papillomavirus type 16-negative head and neck cancers. J Natl Cancer Inst 2008;100:407e20.
7. Lydiatt WM, Patel SG, O'Sullivan B, Brandwein MS, Ridge JA, Migliacci JC, et al. Head and neck cancers-major changes in the American Joint Committee on cancer eighth edition cancer staging manual. CA Cancer J Clin 2017;67:122e37.

8. Kelly JR, Husain ZA, Burtness B. Treatment de-intensification strategies for head and neck cancer. Eur J Cancer 2016;68:125e33.
9. Garcia-Vallve S, Alonso A, Bravo IG. Papillomaviruses: different genes have different histories. Trends Microbiol 2005;13:514e21.
10. Bernard H-U, Burk RD, Chen Z, van Doorslaer K, Hausen H zur, de Villiers E-M. Classification of papillomaviruses (PVs) based on 189 PV types and proposal of taxonomic amendments. Virology. 2010;401(1):70-79. doi:10.1016/j.virol.2010.02.002.
11. de Villiers E-M, Fauquet C, Broker TR, Bernard H-U, zur Hausen H. Classification of papillomaviruses. Virology. 2004;324(1):17-27. doi:10.1016/j.virol.2004.03.033.
12. de Villiers EM. Cross-roads in the classification of papillomaviruses. Virology 2013;445:2e10.
13. Bouvard V, Baan R, Straif K, Grosse Y, Secretan B, El Ghissassi F, et al. A review of human carcinogensePart B: biological agents. Lancet Oncol 2009;10:321e2.
14. IARC. IARC monographs on the evaluation of carcinogenic risks to humans. Monograph. 2007;89:223–276.
15. Chaturvedi, A.K., Anderson, W.F., Lortet-Tieulent, J. et al, Worldwide trends in incidence rates for oral cavity and oropharyngeal cancers. J Clin Oncol. 2013;31:4550–4559.
16. Doorbar J, Quint W, Banks L, Bravo I, Stoler M, et al. The Biology and Life-Cycle of Human Papillomaviruses. Vaccine. 2012;30S:F55– F70. Vaccine. 2012;30S:F55-F70.
17. Faraji F, Zaidi M, Fakhry C, Gaykalova DA. Molecular mechanisms of human papillomavirus-related carcinogenesis in head and neck cancer. Microbes Infect. 2017;19(9-10):464-475.
18. Tumban E. A Current Update on Human Papillomavirus-Associated Head and Neck Cancers. Viruses. 2019 Oct 9;11(10). pii: E922. doi: 10.3390/v11100922.
19. Finnen RL, Erickson KD, Chen XS, Garcea RL. Interactions between Papillomavirus L1 and L2 Capsid Proteins. J Virol. 2003;77(8):4818-4826. doi:10.1128/jvi.77.8.4818-4826.2003.

20. Münger K, Baldwin A, Edwards KM, et al. Mechanisms of Human Oncogenesis MINIREVIEW Mechanisms of Human Papillomavirus-Induced Oncogenesis. Society. 2004;78(21):11451-11460. doi:10.1128/JVI.78.21.11451.
21. McBride AA. The Papillomavirus E2 proteins. Virology. 2013;445(1-2):57-79. doi:10.1016/j.virol.2013.06.006.
22. Müller M, Prescott EL, Wasson CW, MacDonald A. Human papillomavirus E5 oncoprotein: Function and potential target for antiviral therapeutics. Future Virol. 2015;10(1):27-39. doi:10.2217/fvl.14.99.
23. Krawczyk E, Suprynowicz FA, Liu X, et al. A cooperative interaction between the human papillomavirus E5 and E6 oncoproteins. Am J Pathol. 2008;173(3):682-688. doi:10.2353/ajpath.2008.080280.
24. Yajid AI, Zakariah MA, Zin AAM, Othman NH. Potential role of E4 protein in human papillomavirus screening: A review. Asian Pacific J Cancer Prev. 2017;18(2):315-319. doi:10.22034/APJCP.2017.18.2.315.
25. Castellsague X, Alemany L, Quer M, Halec G, Quiros B, Tous S, et al. HPV involvement in head and neck cancers: comprehensive assessment of biomarkers in 3680 patients. J Natl Cancer Inst 2016;108. djv403.
26. Riethdorf S, Neffen EF, Cviko A, Loning T, Crum CP, Riethdorf L. p16INK4A expression as biomarker for HPV 16-related vulvar neoplasias. Hum Pathol 2004;35:1477e83.
27. Kines RC, Thompson CD, Lowy DR, Schiller JT, Day PM. The initial steps leading to papillomavirus infection occur on the basement membrane prior to cell surface binding. Proc Natl Acad Sci U. S. A 2009;106:20458e63.
28. Perry ME. The specialised structure of crypt epithelium in the human palatine tonsil and its functional significance. J Anat 1994;185(Pt 1):111e27.

29. Pyeon D, Pearce SM, Lank SM, Ahlquist P, Lambert PF. Establishment of human papillomavirus infection requires cell cycle progression. PLoS Pathog 2009;5:e1000318.
30. Bravo IG, Fe´lez-Sanchez M. Papillomaviruses: viral evolution, cancer and evolutionary medicine. Evol Med Public Health 2015; 2015(1):32–51.
31. Taberna M, Mena , Pavón MA, Alemany L, Gillison ML, Mesía R. Human papillomavirus-related oropharyngeal cancer. Ann Oncol. 2017 Oct 1;28(10):2386-2398.
32. Pannone G, Rodolico V, Santoro A et al. Evaluation of a combined triple method to detect causative HPV in oral and oropharyngeal squamous cell carcinomas: p16 immunohistochemistry, consensus PCR HPV-DNA, and in situ hybridization. Infect Agent Cancer 2012; 7(1): 4.
33. Leemans CR, Braakhuis BJM, Brakenhoff RH. The molecular biology of head and neck cancer. Nat Rev Cancer 2011; 11(1): 9–22.
34. Huang SH, Perez-Ordonez B, Liu F-F et al. Atypical clinical behavior of p16-confirmed HPV-related oropharyngeal squamous cell carcinoma treated with radical radiotherapy. Int J Radiat Oncol Biol Phys 2012; 82(1): 276–283.
35. Peck BW, Dahlstrom KR, Gan SJ et al. Low risk of second primary malignancies among never smokers with human papillomavirus-associated index oropharyngeal cancers. Head Neck 2013; 35(6): 794–799.
36. Rietbergen MM, Braakhuis BJM, Moukhtari N et al. No evidence for active human papillomavirus (HPV) in fields surrounding HPV-positive oropharyngeal tumors. J Oral Pathol Med 2014; 43(2): 137–142.
37. Paver EC, Currie AM, Gupta R, Dahlstrom JE. Human papilloma virus related squamous cell carcinomas of the head and neck: diagnosis, clinical implications and detection of HPV. Pathology. 2020;52(2):179-191. doi:10.1016/j.pathol.2019.10.008

38. Saber CN, Grønhøj Larsen C, Dalianis T, Von Buchwald C. Immune cells and prognosis in HPV-associated oropharyngeal squamous cell carcinomas: review of the literature. Oral Oncol 2016; 58: 8–13.
39. Kim KY, Lewis JS, Chen Z. Current status of clinical testing for human papillomavirus in oropharyngeal squamous cell carcinoma. J Pathol Clin Res 2018; 4: 213–26.
40. Lewis JS Jr, Beadle B, Bishop JA, et al. Human papillomavirus testing in head and neck carcinomas: guideline from the College of American Pathologists. Arch Pathol Lab Med 2018; 142: 559–97.
41. El-Naggar AK, Westra WH. p16 expression as a surrogate marker for HPV-related oropharyngeal carcinoma: a guide for interpretative relevance and consistency. Head Neck 2012; 34: 459–61.
42. Boscolo-Rizzo P, Pawlita M, Holzinger D. From HPV-positive towards HPV-driven oropharyngeal squamous cell carcinomas. Cancer Treatment Reviews 2016;42:24–29.
43. Prigge ES, Arbyn M, von Knebel Doeberitz M, Reuschenbach M. Diagnostic accuracy of p16INK4a immunohistochemistry in oropharyngeal squamous cell carcinomas: a systematic review and metaanalysis. Int J Cancer 2017; 140(5): 1186–1198.
44. Kreimer AR, Johansson M, Waterboer T, Kaaks R, Chang-Claude J, Drogen D, et al. Evaluation of human papillomavirus antibodies and risk of subsequent head and neck cancer. J Clin Oncol 2013;31(21):2708–15.
45. Spector ME et al. E6 and E7 Antibody Levels Are Potential Biomarkers of Recurrence in Patients With Advanced-Stage Human Papillomavirus-Positive Oropharyngeal Squamous Cell Carcinoma. Clin Cancer Res. 2017 Jun 1;23(11):2723-2729.

46. Hanna GJ et al. Salivary and Serum HPV Antibody Levels Before and After Definitive Treatment in Patients With Oropharyngeal Squamous Cell Carcinoma. Cancer Biomark 2017;19(2):129-136.
47. Tang KD et al. Unlocking the Potential of Saliva-Based Test to Detect HPV-16-Driven Oropharyngeal Cancer. Cancers (Basel) 2019 Apr 3;11(4):473.
48. Qureishi, A.; Ali, M.; Fraser, L.; Shah, K.A.; Moller, H.; Winter, S. Saliva testing for human papilloma virus in oropharyngeal squamous cell carcinoma: A diagnostic accuracy study. Clin. Otolaryngol. 2018, 43, 151–157.
49. Tang, K.D.; Kenny, L.; Frazer, I.H.; Punyadeera, C High-risk human papillomavirus detection in oropharyngeal cancers: Comparison of saliva sampling methods. Head Neck 2019 May;41(5):1484-1489.
50. Wang J. Electrochemical biosensors: towards point-of-care cancer diagnostics. Biosens Bioelectron 2006;21:1887–92.
51. Dell'Atti D, Zavaglia M, Tombelli S, Bertacca G. et al. Development of combined DNA-based piezoelectric biosensors for the simultaneous detection and genotyping of high risk Human Papilloma Virus strains. Clinica Chimica Acta 2007;383:140–146.
52. Zhou Y, Chiu CW, Liang H. Interfacial Structures and Properties of Organic Materials for Biosensors: An Overview. Sensors (Basel). 2012 Nov 6;12(11):15036-62.
53. Grieshaber D, MacKenzie R, Vörös J, Reimhult E. Electrochemical Biosensors - Sensor Principles and Architectures. Sensors. 2008;8(3):1400-1458
54. Ronkainen NJ, Halsall HB, Heineman WR. Electrochemical biosensors. Chem Soc Rev. 2010;39(5):1747-1763. doi:10.1039/b714449k.
55. Mioslav, P.; Petr, S. Electrochemical biosensors-principles and applications. J. Appl. Biomed. 2008, 6, 57–64.

56. Wang S, Yin T, Zeng S, Che H, Yang F, Chen X, et al. (2012) A Piezoelectric Immunosensor Using Hybrid Self-Assembled Monolayers for Detection of Schistosoma japonicum. PLoS ONE 7(1): e30779.
57. Thevenot D, Toth K, Durst R, et al. Electrochemical biosensors : recommended definitions and classification To cite this version : Technical report Electrochemical biosensors : recommended definitions and. Biosens Bioelectron. 2001;16:121-131.
58. Silva BVM, I.T. Cavalcanti, A.B. Mattos, P. Moura, M.D.P.T. Sotomayor, R.F. Dutra, Disposable immunosensor for human cardiac troponin T based on streptavidin-microsphere modified screen-printed electrode, Biosensors & Bio- electronics. (2010;26(3):1062–1067.
59. Arya SK, P.R. Solanki, M. Datta, B.D. Malhotra, Recent advances in self- assembled monolayers based biomolecular electronic devices, Biosensors & Bioelectronics 2009;24(9): 2810–2817.
60. Ferguson M, Dianna E. Wilkinson, Alan Heath, and Paul Matejtschuk, 'The First International Standard for Antibodies to HPV 16. Vaccine. 2011;29:6520-26.
61. Ferguson M, Dianna E. Wilkinson, Alan Heath, and Paul Matejtschuk, 'Proposal to Establish the Who Reference Reagent for Antibodies to HPV 16 (05/134) as an International Standard Following Stability Studies', in Expert Committee on Biological StandardizatioN WHO/BS/09.2113 (2009).
62. https://www.jpt.com/?_ga=2.101208451.36784840.1590332286-341636147.1587627368. Protocol PepMix™ for Antigen-specific stimulation of T-Lymphocytes.
63. Yang YS, Smith-McCune K, Darragh TM, et al. Direct human papillomavirus E6 whole-cell enzyme-linked immunosorbent assay for objective measurement of E6 oncoproteins in cytology samples. Clin Vaccine Immunol. 2012;19(9):1474-1479. doi:10.1128/CVI.00388-12.

64. Manea F. Modern Electrochemical Methods in Nano, Surface and Corrosion Science in Electrochemical Techniques for Characterization and Detection Application of Nanostructured Carbon Composite. http://dx.doi.org/10.5772/58633
65. Remes A, Pop A, Manea F, Baciu A, Picken S J, Schoonman J. Electrochemical Determination of Pentachlorophenol in Water on a Multi-Wall Carbon Nanotubes-Epoxy Composite Electrode. Sensors. 2012;12(6): 7033-7046.
66. Wang J. Carbon-Nanotube Based Electrochemical Biosensors: a Review, Electroanal. 2005;17 (1): 7-14.
67. Santos A, Davis JJ, Bueno PR. Fundamentals and applications of impedimetric and redox capacitive biosensors. Journal of Analytical and Bioanalytical Techniques. 2014;S7(016):1-15.
68. Randviir EP, Banks CE. Electrochemical impedance spectroscopy: An overview of bioanalytical applications. Analytical Methods. 2013;5(5):1098.
69. Fischer LM, Tenje M, Heiskanen AR, et al. Gold cleaning methods for electrochemical detection applications. Microelectron Eng. 2009;86(4-6):1282-1285. doi:10.1016/j.mee.2008.11.045.
70. Wrona PK. Solution : 2005:2005.
71. Colorado R J, Lee TR, in Encyclopedia of Materials: Science and Technology, 2001.
72. Ramos CA, Narala N, Vyas GM, Leen AM, Gerdemann U, Sturgis EM, Anderson ML, Savoldo B, Heslop HE, Brenner MK, Rooney CM. Human Papillomavirus Type 16 E6/E7-specific Cytotoxic T Lymphocytes for Adoptive Immunotherapy of HPV-associated Malignancies. J Immunother. 2013 Jan;36(1):66-76.
73. Illiano E, Demurtas OC, Massa S, et al. Production of functional, stable, unmutated recombinant human papillomavirus E6 oncoprotein: implications for HPV-tumor diagnosis and therapy. J Transl Med. 2016;14(1):224.

74. Frederix F, Bonroy K, Laureyn W, Reekmans G, Campitelli A, et al. Enhanced Performance of an Affinity Biosensor Interface Based on Mixed Self-Assembled Monolayers of Thiols on Gold. Langmuir 2003;19: 4351–4357.
75. Anantharaman D, Billot A, Waterboer T, et al. Predictors of oropharyngeal cancer survival in Europe. Oral Oncol. 2018;81:89-94.
76. Schroeder L, Wichmann G, Willner M, Michel A, Wiesenfarth M, Flechtenmacher C, Gradistanac T, Pawlita M, Dietz A, Waterboer T, Holzinger D. Antibodies against human papillomaviruses as diagnostic and prognostic biomarker in patients with neck squamous cell carcinoma from unknown primary tumor. Int J Cancer. 2018 Apr 1;142(7):1361-1368.
77. Kreimer AR, Johansson M, Yanik EL, et al. Kinetics of the Human Papillomavirus Type 16 E6 Antibody Response Prior to Oropharyngeal Cancer. J Natl Cancer Inst. 2017;109(8):djx005. doi:10.1093/jnci/djx005
78. Kreimer AR, Ferreiro-Iglesias A, Nygard M, et al. Timing of HPV16-E6 antibody seroconversion before OPSCC: findings from the HPVC3 consortium. Ann Oncol. 2019;30(8):1335-1343. doi:10.1093/annonc/mdz138
79. Kreimer AR, Chaturvedi AK, Alemany L, et al. Summary from an international cancer seminar focused on human papillomavirus (HPV)-positive oropharynx cancer, convened by scientists at IARC and NCI. [published online ahead of print, 2020 Jun 2]. Oral Oncol. 2020;108:104736. doi:10.1016/j.oraloncology.2020.104736
80. D'Souza G, Gross ND, Pai SI, Haddad R, Anderson KS, Rajan S, et al. Oral human papillomavirus (HPV) infection in HPV-positive patients with oropharyngeal cancer and their partners. J Clin Oncol. 2014;32:2408-2415.

81. Dahlstrom KR, Anderson KS, Cheng JN, et al. HPV Serum Antibodies as Predictors of Survival and Disease Progression in Patients with HPV-Positive Squamous Cell Carcinoma of the Oropharynx. Clin Cancer Res. 2015;21(12):2861-2869. doi:10.1158/1078-0432.CCR-14-3323
82. Wang Y, Feng J, Tan Z, Wang H. Electrochemical impedance spectroscopy aptasensor for ultrasensitive detection of adenosine with dual backfillers. Biosens Bioelectron. 2014;60:218-223. doi:10.1016/j.bios.2014.04.022
83. Wang S, Li L, Jin H, et al. Electrochemical detection of hepatitis B and papilloma virus DNAs using SWCNT array coated with gold nanoparticles. Biosens Bioelectron. 2013;41:205-210. doi:10.1016/j.bios.2012.08.021
84. Nasirizadeh N, Zare HR, Pournaghi-Azar MH, Hejazi MS. Introduction of hematoxylin as an electroactive label for DNA biosensors and its employment in detection of target DNA sequence and single-base mismatch in human papilloma virus corresponding to oligonucleotide. Biosens Bioelectron. 2011;26(5):2638-2644. doi:10.1016/j.bios.2010.11.026.